

Supporting Information

for

**Synthesis, X-ray structure and magnetic properties of the apically  
functionalized monocapped cobalt(II) tris-pyridineoximates possessing a  
SMM behaviour**

Alexander S. Belov,<sup>a,b</sup> Svetlana A. Belova,<sup>a,b</sup> Nikolay N. Efimov,<sup>a</sup> Veronika V. Zlobina,<sup>b</sup> Valentin V. Novikov,<sup>c</sup> Yulya V. Nelyubina,<sup>b,d</sup> Yan V. Zubavichus,<sup>e</sup> Yan Z. Voloshin,<sup>a,b</sup> Alexander A. Pavlov<sup>b,d,f\*</sup>

<sup>a</sup>Kurnakov Institute of General and Inorganic Chemistry of the Russian Academy of Sciences, 31 Leninsky pr., 119991 Moscow, Russia

<sup>b</sup>Nesmeyanov Institute of Organoelement Compounds of the Russian Academy of Sciences, 28-1 Vavilova st., 119334 Moscow, Russia

<sup>c</sup>Moscow Institute of Physics and Technology, National Research University, Institutskiy per. 9, Dolgoprudny, 141700 Moscow Region, Russia

<sup>d</sup>BMSTU Center of National Technological Initiative "Digital Material Science: New Material and Substances", Bauman Moscow State Technical University, 2nd Baumanskaya st. 5, 105005, Moscow, Russia

<sup>e</sup>Synchrotron Radiation Facility SKIF, G.K. Boreskov Institute of Catalysis of the Siberian Branch of the Russian Academy of Sciences, 1 Nikolskii pr., 630559 Koltsovo, Russia

<sup>f</sup>National Research University Higher School of Economics, 101000 Moscow, Russia

## Experimental

### *Materials and methods*

The reagents used,  $\text{FeCl}_2 \cdot 4\text{H}_2\text{O}$ ,  $\text{Co}(\text{ClO}_4)_2 \cdot 6\text{H}_2\text{O}$ , 4-(bromomethyl)phenylboronic acid, ferrocenylboronic acid, sodium methylthiosulfonate,  $\text{NaHCO}_3$ ,  $\text{NaClO}_4 \cdot \text{H}_2\text{O}$ ; sorbents and organic solvents, were obtained commercially (SAF®). 2-acetylpyridineoxime ligand *AcPyOxH* was prepared as described elsewhere [S1].

Analytical data (C, H, N contents) were obtained with a Carlo Erba model 1106 microanalyzer. The iron and cobalt contents were determined by the X-ray fluorescence method.

MALDI-TOF mass spectra were recorded in both the positive and negative spectral ranges using a MALDI-TOF-MS Bruker Autoflex mass spectrometer in reflecto-mol mode. The ionization was induced by UV-laser with wavelength 336 nm. The samples were applied to a nickel plate, 2,5-dihydroxybenzoic acid was used as a matrix. The accuracy of measurements was 0.1%.

UV-Vis spectra of the solutions in dichloromethane were recorded in the range 230 – 800 nm with a Varian Cary 60 spectrophotometer. The individual Gaussian components of these spectra were calculated using the Fityk program [S2].

$^1\text{H}$  and  $^{13}\text{C}\{^1\text{H}\}$  NMR spectra were recorded from the solutions in  $(\text{CD}_3)_2\text{SO}$  and  $\text{CD}_2\text{Cl}_2$  with a Bruker Avance 300, Avance 600 FT-spectrometer and Varian Inova 400 spectrometer.

Magnetic susceptibility was measured in the temperature range 3 – 300 K with a Quantum Design PPMS-9 device under the DC magnetic field of 1 kOe. The corresponding finely ground fine-crystalline sample was immobilized in mineral oil matrix inside a polyethylene capsule. The data were corrected for the sample holder, the mineral oil and the diamagnetic contribution; the latter by using the

Pascal constants. The oscillating ac fields of 1 Oe with the frequencies in the range from 10 to 10000 Hz were employed for the AC magnetometry.

## ***Synthesis***

### *Synthesis of 4-(methylthiosulfonatomethyl)phenylboronic acid*

4-Bromomethylphenylboronic acid (0.50 g, 2.34 mmol) and sodium methylthiosulfonate (0.36 g, 3.51 mmol) were dissolved/suspended in methanol (10 ml), the reaction mixture was refluxed for 30 min, then cooled to r.t., evaporated to a small volume (approximately 1 ml) and precipitated with diethyl ether (10 ml). The precipitate was filtered off, washed with diethyl ether (5 ml) and dried *in vacuo*. Yield: 0.18 g (37%). <sup>1</sup>H NMR ((CD<sub>3</sub>)<sub>2</sub>SO) δ, ppm: 3.16 (s, 3H, CH<sub>3</sub>), 4.48 (s, 2H, CH<sub>2</sub>), 7.38 (dd, 2H, *ortho*-Ph), 7.78 (d, 2H, *meta*-Ph). <sup>13</sup>C {<sup>1</sup>H} NMR ((CD<sub>3</sub>)<sub>2</sub>SO) δ, ppm: 39.58 (s, CH<sub>3</sub>), 50.42 (s, CH<sub>2</sub>), 128.28 (s, *ortho*-Ph), 134.59 (s, *meta*-Ph), 137.10 (s, *ipso*-Ph).

### *Synthesis of the pseudoclathrochelate complexes*

#### **1: [Co(AcPyOx)<sub>3</sub>(BC<sub>6</sub>H<sub>4</sub>CH<sub>2</sub>Br)](ClO<sub>4</sub>).**

2-Acetylpyridineoxime (0.32 g, 2.35 mmol), NaHCO<sub>3</sub> (0.28 g, 3.35 mmol) and 4-bromomethylphenylboronic acid (0.17 g, 0.80 mmol) were dissolved in ethanol (4 ml) under argon. Then, Co(ClO<sub>4</sub>)<sub>2</sub>·6H<sub>2</sub>O (0.25 g, 0.67 mmol) and ethanol (1 ml) were added to the obtained solution under stirring. The reaction mixture was refluxed for 1h, cooled to r.t. and the orange precipitate formed was filtered off. The product was washed with ethanol (12 ml, in four portions), diethyl ether (10 ml, in two portions) and hexane (5 ml), and extracted with dichloromethane (30 ml, in six portion). The extract was filtered, evaporated to dryness, and the solid residue was dried *in vacuo*. Yield: 0.28 g (55%). Anal. Calc. for C<sub>28</sub>H<sub>27</sub>N<sub>6</sub>O<sub>7</sub>BClBrCo (%): C, 45.13; H, 3.63; N, 11.28; Co, 7.92. Found (%): C, 44.28; H, 3.42; N, 10.85; Co, 8.00. MS (MALDI-TOF): *m/z*: 645 [M – ClO<sub>4</sub><sup>-</sup>]<sup>+</sup>. <sup>1</sup>H NMR (CD<sub>2</sub>Cl<sub>2</sub>) δ, ppm: -2.84 (br. s, 3H, 3-Py), 2.21 (br. s, 9H, CH<sub>3</sub>), 14.82 (br. s, 3H, 4-Py), 18.38 (br. s, 2H, *Br*-CH<sub>2</sub>), 30.41 (br. s, 2H, *meta*-Ph), 68.30 (br. s, 2H,

*ortho*-Ph), 80.40 (br. s, 3H, 5-Py), 397.93 (br. s, 3H, 6-Py). Deconvoluted UV-Vis (CH<sub>2</sub>Cl<sub>2</sub>):  $\nu$ , cm<sup>-1</sup> ( $\epsilon \times 10^{-3}$ , mol<sup>-1</sup>L cm<sup>-1</sup>): 40320(35), 34600(7.7), 32895(7.3), 30210(5.5), 27700(1.9), 26600(0.63), 23095(0.26).

**2: [Fe(AcPyOx)<sub>3</sub>(BC<sub>6</sub>H<sub>4</sub>CH<sub>2</sub>Br)](ClO<sub>4</sub>).**

2-Acetylpyridineoxime (0.32 g, 2.36 mmol), NaClO<sub>4</sub>·H<sub>2</sub>O (0.47 g, 3.37 mmol), NaHCO<sub>3</sub> (0.17 g, 2.02 mmol) and 4-bromomethylphenylboronic acid (0.22 g, 1.01 mmol) were dissolved in ethanol (3 ml) under argon. The reaction mixture was stirred for 5 min and FeCl<sub>2</sub>·4H<sub>2</sub>O (0.13 g, 0.67 mmol) and ethanol (1 ml) were added. The reaction mixture was refluxed for 2h, cooled to r.t. and the dark-red precipitate formed was filtered off. The product was washed with ethanol (15 ml, in three portions), diethyl ether (10 ml, in two portions) and hexane (5 ml) and, then, it was extracted with dichloromethane (6 ml, in two portions). The extract was filtered, evaporated to dryness and the solid residue was dried *in vacuo*. Yield: 0.33 g (66%). Anal. Calc. for C<sub>28</sub>H<sub>27</sub>N<sub>6</sub>O<sub>7</sub>BClBrFe (%): C, 45.31; H, 3.64; N, 11.33; Fe, 7.55. Found (%): C, 44.98; H, 3.64; N, 11.16; Fe, 8.30. MS (MALDI-TOF):  $m/z$ : 642 [M – ClO<sub>4</sub><sup>-</sup>]<sup>+</sup>. <sup>1</sup>H NMR (CD<sub>2</sub>Cl<sub>2</sub>)  $\delta$ , ppm: 2.66 (s, 9H, CH<sub>3</sub>), 4.58 (s, 2H, CH<sub>2</sub>), 7.06 (d, 3H, 6-Py), 7.43 (d, 2H, *meta*-Ph), 7.51 (t, 3H, 5-Py), 7.75 (d, 2H, *ortho*-Ph) 7.96 (d, 3H, 3-Py), 8.06 (t, 3H, 4-Py). <sup>13</sup>C{<sup>1</sup>H} NMR (CD<sub>2</sub>Cl<sub>2</sub>)  $\delta$ , ppm: 13.80 (s, CH<sub>3</sub>), 35.00 (s, CH<sub>2</sub>Br), 125.16 (s, 3-Py), 126.35 (s, 5-Py), 128.68 (s, *meta*-Ph), 132.76 (s, *ortho*-Ph), 138.02 (s, (C-CH<sub>2</sub>)), 138.53 (s, 4-Py), 153.47 (s, 6-Py), 158.53 (s, C=N), 161.25 (s, C=N). Deconvoluted UV-Vis (CH<sub>2</sub>Cl<sub>2</sub>):  $\nu$ , cm<sup>-1</sup> ( $\epsilon \times 10^{-3}$ , mol<sup>-1</sup>L cm<sup>-1</sup>): 39530(13), 38310(4.3), 35460(16), 33780(16), 33560(6.4), 28250(4.4), 25970(0.9), 23360(1.2), 20530(4.0), 20200(8.2), 19010(12).

**3: [Co(AcPyOx)<sub>3</sub>(BC<sub>6</sub>H<sub>4</sub>CH<sub>2</sub>SSO<sub>2</sub>CH<sub>3</sub>)](ClO<sub>4</sub>).**

2-Acetylpyridineoxime (0.11 g, 0.78 mmol), NaHCO<sub>3</sub> (0.07 g, 0.78 mmol) and 4-(methylthiosulfonatomethyl)phenylboronic acid (0.06 g, 0.28 mmol) were dissolved in ethanol (2 ml) under argon. Then, Co(ClO<sub>4</sub>)<sub>2</sub>·6H<sub>2</sub>O (0.10 g, 0.26 mmol) and ethanol (2 ml) were added to the obtained solution under stirring. The reaction mixture was stirred for 1h at r.t. and the yellow precipitate formed was

filtered off. The product was washed with ethanol (8 ml, in four portions) and diethyl ether (10 ml, in two portions), and, then, extracted with dichloromethane (6 ml, in two portion). The extract was filtered, evaporated to dryness and the solid residue was dried *in vacuo*. Yield: 0.13 g (63%). Anal. Calc. for  $C_{29}H_{30}N_6O_9BS_2ClCo$  (%): C, 44.87; H, 3.87; N, 10.83; Co, 7.61. Found (%): C, 44.98; H, 3.73; N, 10.77; Co, 7.90. MS (MALDI-TOF):  $m/z$ : 676  $[M - ClO_4^-]^+$ .  $^1H$  NMR ( $CD_2Cl_2$ )  $\delta$ , ppm: -2.37 (br. s, 3H, 3-Py), 2.48 (br. s, 9H,  $CH_3$ ), 13.50 (br. s, 3H,  $CH_3$ ), 15.37 (br. s, 3H, 4-Py), 18.15 (br. s, 2H,  $CH_2$ ), 30.23 (br. s, 2H, *meta*-Ph), 68.21 (br. s, 2H, *ortho*-Ph), 80.71 (br. s, 3H, 5-Py), 398.74 (br. s, 3H, 6-Py). Deconvoluted UV-Vis ( $CH_2Cl_2$ ):  $\nu$ ,  $cm^{-1}$  ( $\epsilon \times 10^{-3}$ ,  $mol^{-1}L\ cm^{-1}$ ): 39680(15), 34840(14), 34600(4.3), 28170(3.1), 24810(0.27), 22990(0.23).

#### **4: $[Fe(AcPyOx)_3(BC_6H_4CH_2SSO_2CH_3)](ClO_4)$**

##### *Method 1*

2-Acetylpyridineoxime (0.11 g, 0.78 mmol),  $NaClO_4 \cdot H_2O$  (0.11 g, 0.78 mmol),  $NaHCO_3$  (0.07 g, 0.78 mmol) and 4-(methylthiosulfonatomethyl)phenylboronic acid (0.06 g, 0.28 mmol) were dissolved in ethanol (2 ml) under argon. Then,  $FeCl_2 \cdot 4H_2O$  (0.52 g, 0.26 mmol) and ethanol (1 ml) were added to the obtained solution under stirring. The reaction mixture was refluxed for 1h, cooled to r.t. and the dark-red precipitate formed was filtered off. The product was washed with ethanol (9 ml, in three portions) and diethyl ether (15 ml, in three portions), and, extracted with dichloromethane (10 ml, in three portion). The extract was filtered, evaporated to dryness and the solid residue was dried *in vacuo*. Yield: 0.09 g (45%).

##### *Method 2*

Complex  $[Fe(AcPyOx)_3(BC_6H_4CH_2Br)](ClO_4)$  (0.05 g, 0.07 mmol) and sodium methylthiosulfonate (0.01 g, 0.10 mmol) were dissolved in methanol (2.5 ml) under argon. The reaction mixture was refluxed for 2h, cooled to r.t. and evaporated to dryness. The dark-red precipitate formed was filtered, washed with diethyl ether (10 ml, in two portions) and, then, extracted with dichloromethane (9 ml, in three portions). The extract was filtered, evaporated to dryness and the solid

residue was dried *in vacuo*. Yield: 0.04 g (84%). Anal. Calc. for  $C_{29}H_{30}N_6O_9BS_2ClFe$  (%): C, 45.05; H, 3.88; N, 10.87. Found (%): C, 44.94; H, 4.04; N, 10.71. MS (MALDI-TOF):  $m/z$ : 673  $[M - ClO_4^-]^+$ .  $^1H$  NMR ( $CD_2Cl_2$ )  $\delta$ , ppm: 2.66 (s, 9H,  $CH_3$ ), 3.07 (s, 3H,  $CH_3$ ), 4.43 (s, 2H,  $CH_2$ ), 7.05 (d, 3H, 6-Py), 7.43 (d, 2H, *meta*-Ph), 7.51 (t, 3H, 5-Py), 7.78 (d, 2H, *ortho*-Ph), 7.96 (d, 3H, 3-Py), 8.06 (t, 3H, 4-Py).  $^{13}C\{^1H\}$  NMR ( $CD_2Cl_2$ )  $\delta$ , ppm: 13.80 (s, Py- $CH_3$ ), 41.51 (s,  $CH_3$ ), 51.43 (s,  $CH_2Br$ ), 125.16 (s, 3-Py), 126.36 (s, 5-Py), 128.78 (s, *meta*-Ph), 132.95 (s, *ortho*-Ph), 134.91 (s, ( $\underline{C}$ - $CH_2$ )), 138.53 (s, 4-Py), 153.48 (s, 6-Py), 158.51, 161.24 (s, C=N). Deconvoluted UV-Vis ( $CH_2Cl_2$ ):  $\nu$ ,  $cm^{-1}$  ( $\epsilon \times 10^{-3}$ ,  $mol^{-1}L\ cm^{-1}$ ): 39840(18), 38310(5.0), 35590(11), 34130(14), 33560(3.9), 28490(3.8), 26040(0.8), 23530(0.4), 20580(3.8), 20410(5.7), 19050(11).

#### **5: $[Co(AcPyOx)_3(BFc)](ClO_4)$ .**

For the first time, the preparation and spectral characterization of this complex have been performed [S11].

2-Acetylpyridineoxime (0.27 g, 1.98 mmol),  $NaClO_4 \cdot H_2O$  (0.18 g, 1.3 mmol),  $NaHCO_3$  (0.28 g, 3.3 mmol) and ferrocenylboronic acid (0.17 g, 0.73 mmol) were dissolved/suspended in ethanol (3 ml) under argon. This solution was stirred for 5 min and  $Co(ClO_4)_2 \cdot 6H_2O$  (0.24 g, 0.66 mmol) and ethanol (4 ml) were added under stirring. The reaction mixture was refluxed for 40 min and the pale-yellow precipitate formed was filtered off. The product was washed with ethanol (30 ml, in six portions), diethyl ether (10 ml, in two portions) and hexane (5 ml), and, then, extracted with dichloromethane (20 ml, in four portions). The extract was filtered, evaporated to dryness and the solid residue was dried *in vacuo*. Yield: 0.26 g (52%). Anal. Calc. for  $C_{31}H_{30}N_6O_7BClCoFe$  (%): C, 48.98; H, 3.95; N, 11.06; Fe, 7.37; Co, 7.77. Found (%): C, 48.79; H, 3.88; N, 10.97; Fe, 7.25; Co, 7.60. MS (MALDI-TOF):  $m/z$ : 660  $[M - ClO_4^-]^+$ .  $^1H$  NMR ( $CD_2Cl_2$ )  $\delta$ , ppm: -2.78 (br. s, 3H, 3-Py), 2.53 (br. s, 9H,  $CH_3$ ), 14.62 (br. s, 3H, 4-Py), 24.87 (br. s, 5H, Cp (unsubstituted)), 27.20 (br. s, 2H,  $\beta$ -Cp), 56.67 (br. s, 2H,  $\alpha$ -Cp), 80.35 (br. s, 3H, 5-Py), 397.23 (br. s, 3H, 6-Py). Deconvoluted UV-Vis ( $CH_3CN$ ):  $\nu$ ,  $cm^{-1}$  ( $\epsilon \times 10^{-3}$ ,

mol<sup>-1</sup>L cm<sup>-1</sup>): 49750(48), 45250(25), 40160(8.6), 38170(2.7), 36100(15), 29325(5.3), 24100(0.6), 23470(0.8).

### ***Single crystal XRD experiments***

Single crystals of the complexes **1**, **3** and **5** were grown at room temperature from their saturated solutions in dichloromethane – hexane (**1** and **3**) and benzene – *iso*-octane (**5**) mixtures, respectively. Intensities of the reflections for **1** and **3** were collected at 100.0(2) K at the “Belok” beamline of the Kurchatov Synchrotron Radiation Source [S3 and S4] at a wavelength of 0.96990 Å using a MAR CCD 165 detector. Intensities of the reflections for **5** were measured on a Bruker Quest diffractometer using Mo-K $\alpha$  radiation ( $\lambda = 0.71073$  Å). Data integration was carried out using the iMosflm software from the CCP4 software suite.[S5] A multi-scan empirical absorption correction was applied to the experimental data using the SCALA program package.[S6] The structures were solved using the intrinsic phasing modification of direct methods as implemented in the SHELXT code[S7] and refined by a full-matrix least squares method against F<sup>2</sup> of all data using the SHELXL-2014[S8] and visualized with the OLEX2[S9] software. Non-hydrogen atoms were refined in the anisotropic approximation. The positions of hydrogen atoms were calculated and included in the refinement in an isotropic approximation by the riding model with the  $U_{\text{iso}}(\text{H}) = 1.5U_{\text{eq}}(\text{C})$  for methyl groups and  $1.2U_{\text{eq}}(\text{C})$  for other atoms, where  $U_{\text{eq}}(\text{X})$  are equivalent thermal parameters of the parent atoms. Experimental details and the results of these refinements are compiled in Table S1. Crystallographic information files are available from the Cambridge Crystallographic Data Center upon a request (<https://ccdc.cam.ac.uk/structure>, deposition numbers are 2217890, 2220567 and 2216782 for **1**, **3**, and **5**, respectively).

### ***Preparation of the apically functionalized monocapped metal(II) tris-pyridineoximate***

Two alternative synthetic pathways towards the target paramagnetic cobalt(II) pseudoclathrochelate [Co(AcPyOx)<sub>3</sub>(BC<sub>6</sub>H<sub>4</sub>CH<sub>2</sub>SSO<sub>2</sub>CH<sub>3</sub>)](ClO<sub>4</sub>), the molecule of

which is decorated with a functionalizing terminal methanethiosulfonate group in the apical substituent, and its diamagnetic iron(II)-centered analog were developed and compared. Both these approaches based on the template condensation on the corresponding  $M^{2+}$  ion as a matrix are shown in Scheme 1. First of them (Scheme 1, Pathway **A**) also includes a post-synthetic transformation (Scheme 2, **II**) of the suitable bromine-terminated metal(II)-encapsulating pseudomacrobicyclic precursor that is formed by a cross-linking with 4-bromomethylphenylboronic acid (Scheme 1, **I**). Contrary, the second synthetic approach (Scheme 1, Pathway **B**) includes an initial isolation of the suitable methanethiosulfonate-containing boronic acid, which then was used as a Lewis-acidic capping agent in the direct template coordination-driven assembly of the target apically functionalized monocapped metal(II) complexes. 4-(methylthiosulfonato)methylphenylboronic acid was obtained in the moderate yield of approximately 50% by nucleophilic substitution of its reactive precursor, 4-bromomethylphenylboronic acid, with sodium methylthiosulfonate as a nucleophilic agent, in methanol (Scheme 1, **III**). On the next stage, the template condensation of thus obtained functionalized boronic acid with three molecules of 2-acetylpyridineoxime on the corresponding metal(II) ion ( $Fe^{2+}$  or  $Co^{2+}$ ) as a matrix in ethanol as a solvent (Scheme 1, **IV**) gave after reflux of the reaction mixture the target cage complexes **3** and **4** in the reasonable yields (42 and 60%, respectively). In the case of the former synthetic approach, the same template condensation with 4-bromomethylphenylboronic acid as a cross-linking agent was used for preparation of the reactive bromine-terminated pseudoclathrochelate precursors **1** and **2** (Scheme 1, **I**), which were isolated under the same reaction conditions with the similar moderate yields (approximately 50 – 60%). Then their further nucleophilic substitution with sodium methylthiosulfonate (Scheme 1, **II**) was performed in methanol. Because of a low solubility of the corresponding pseudomacrobicyclic precursors in a given solvent, the reaction course was thoroughly monitored by TLC method controlling a consumption of this nucleophilic agent. As a result, the target iron(II) complex **4** was obtained in the relatively high yield (84%). On the other hand, its cobalt(II)-

centered analog **3** was found to undergo the side chemical transformations under the same reaction conditions (including the redox processes and the complete decomposition reaction). Therefore, the target cobalt(II) pseudoclathrochelate was isolated in a substantially lower yield. So, in the case of the iron(II) complex of this type, the Pathway **A** that is based on the post-synthetic functionalization of its initially obtained monocapped bromine-terminated precursor, is more favorable synthetic approach, while the direct template condensation of the suitable functionalized boronic acid (Pathway **B**) allowed to obtain its target cobalt(II)-centered analog in a substantially higher total yield.

### *Spectral characterization*

MALDI-TOF mass spectra of the obtained ionic associates contain in the positive range the peaks of the corresponding monocapped metal(II)-centered tris-pyridineoximate monocations (Figs. S11 – S14). These peaks have the characteristic isotopic distributions, which are in good agreement with those theoretically calculated.

Deconvoluted UV-vis spectra of the obtained diamagnetic iron(II) tris-pyrazoloximate pseudoclathrochelates (Figs. S15 – S18) contain in their visible range three less intensive ( $\epsilon \sim 0.4 \div 8 \cdot 10^3 \text{ mol}^{-1}\text{L cm}^{-1}$ ) bands with maxima from approximately 20000 to 25000  $\text{cm}^{-1}$  and one more intensive bond ( $\epsilon \sim 1.1 \div 1.2 \cdot 10^4 \text{ mol}^{-1}\text{L cm}^{-1}$ ) with maximum close to 19000  $\text{cm}^{-1}$ . All these bands were assigned to the metal-to-ligand  $\text{Fed}^6 \rightarrow \text{L}\pi^*$  charge transfers (MLCTs<sup>S10</sup>), while a series of the intensive bands in the UV-range of these spectra was assigned to the  $\pi-\pi^*$  transitions in the chelating pyridineoximate fragments of the monocapped tripodal  $N_6$ -hexadentate ligands and to those of the same nature in their apical substituent as well. UV-vis spectra of the obtained paramagnetic cobalt(II)-centered pseudoclathrochelates, formed by the same pseudomacrobicyclic ligands, contain two substantially lesser intensive ( $\epsilon \sim 2 \div 6 \cdot 10^2 \text{ mol}^{-1}\text{L cm}^{-1}$ )  $\text{Cod}^7 \rightarrow \text{L}\pi^*$  MLCTs bands in their visible and near-UV range in the range 23000 – 27000  $\text{cm}^{-1}$ .

The intensive bands assigned to the ligand-centered  $\pi-\pi^*$  transitions are observed in these spectra in their far-UV ranges.

### ***Crystal structure description***

The compounds **1** and **3** were isolated as solvates with dichloromethane (one solvent molecule per formula unit), whereas the compound **5** was isolated as a solvate with benzene (2.5 molecules per formula unit). The compound **1** is crystallized in the monoclinic  $P2_1/c$  space group, compounds **3** and **5** are crystallized in the triclinic space group  $P-1$ . In all three structures, both the apically functionalized boron-capped cobalt(II) tris-pyridineoximate pseudoclathrochelate cations and  $\text{ClO}_4^-$  anions occupy general positions. In all cases, the cobalt(II) ions adopt a strongly distorted trigonal prismatic coordination environment formed by six nitrogen atoms (three oxime ones and three pyridine ones). Sketches of molecular structures of **1**, **3**, and **5** are shown in Figs S20–S22. Essential geometrical parameters of the common functional cores therein are summarized in Table S2.

All three structures are island-like and form no notable intermolecular contacts.

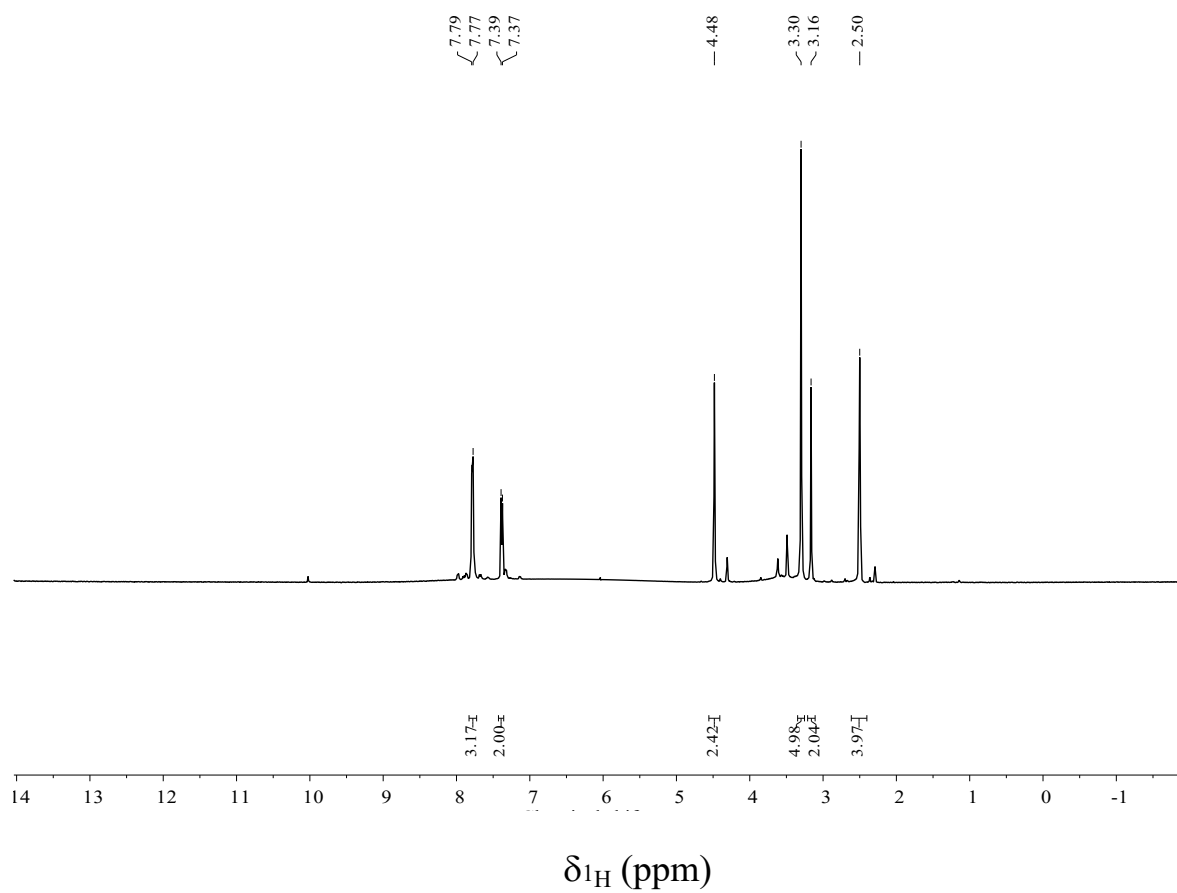


**Figure S1.** Solution  $^1\text{H}$  NMR spectrum of 4-(methylthiosulfonatomethyl)phenylboronic acid in  $\text{DMSO-d}_6$ .

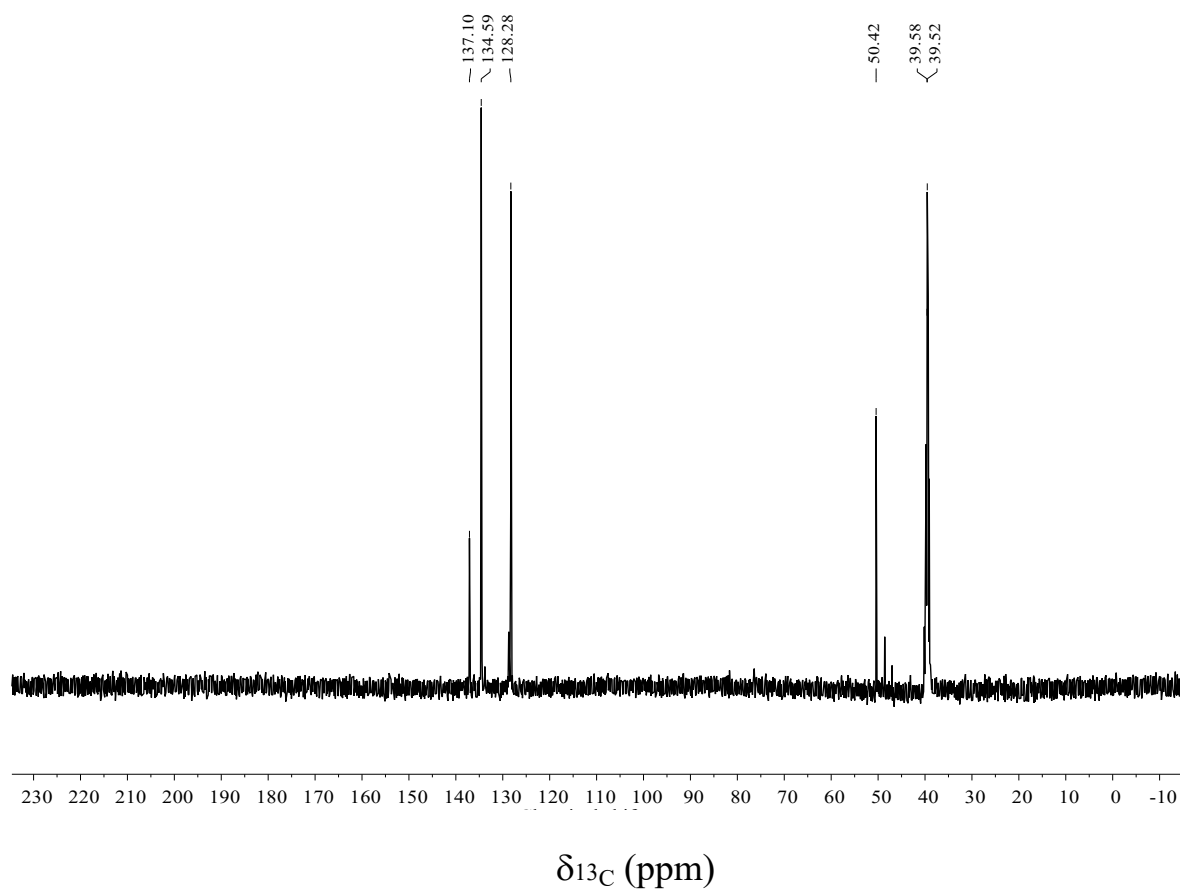


**Figure S2.** Solution  $^{13}\text{C}\{^1\text{H}\}$  NMR spectrum of 4-(methylthiosulfonatomethyl)phenylboronic acid in  $\text{DMSO-d}_6$ .

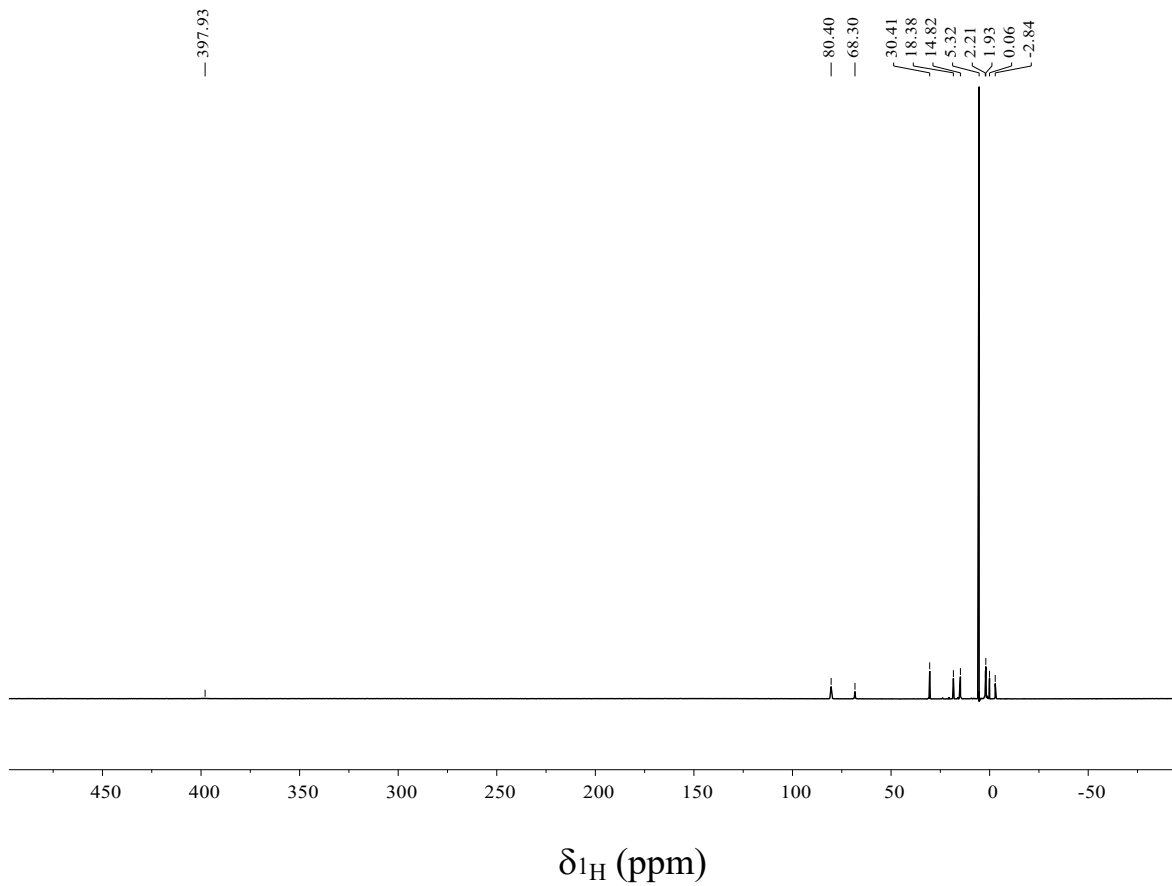


**Figure S3.** Solution  $^1\text{H}$  NMR spectrum of the complex  $[\text{Co}(\text{AcPyOx})_3(\text{BC}_6\text{H}_4\text{CH}_2\text{Br})](\text{ClO}_4)$  (**1**) in  $\text{CD}_2\text{Cl}_2$

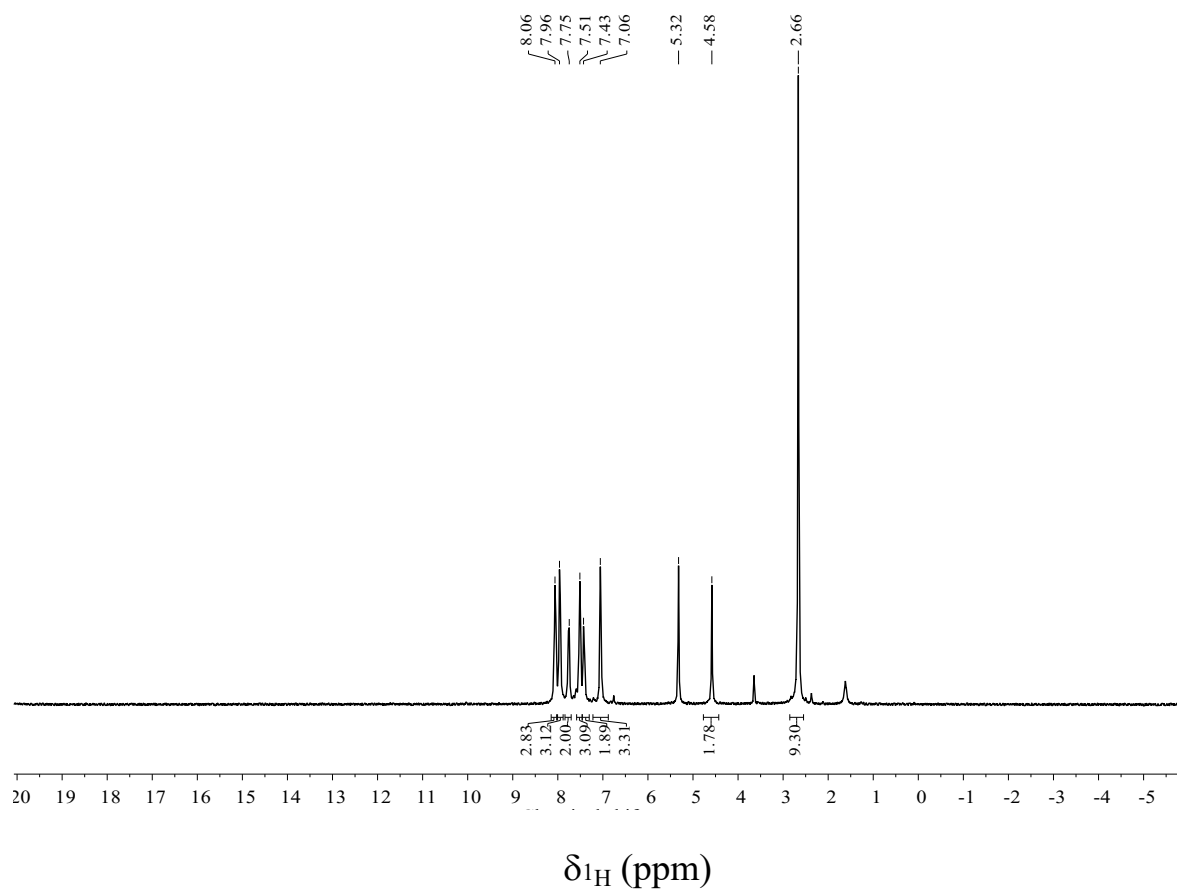


**Figure S4.** Solution  $^1\text{H}$  NMR spectrum of the complex  $[\text{Fe}(\text{AcPyOx})_3(\text{BC}_6\text{H}_4\text{CH}_2\text{Br})](\text{ClO}_4)$  (**2**) in  $\text{CD}_2\text{Cl}_2$

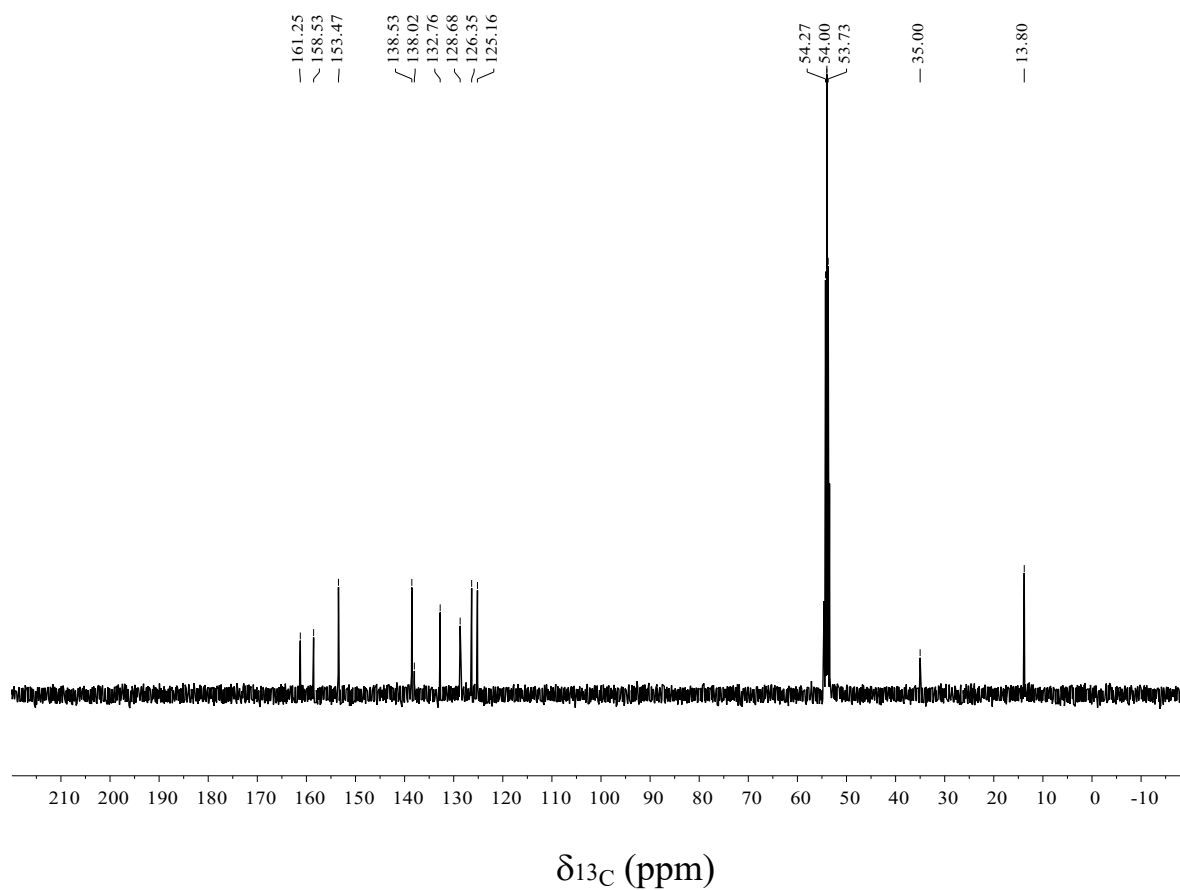


**Figure S5.** Solution  $^{13}\text{C}\{^1\text{H}\}$  NMR spectrum of the complex  $[\text{Fe}(\text{AcPyOx})_3(\text{BC}_6\text{H}_4\text{CH}_2\text{Br})](\text{ClO}_4)$  (**2**) in  $\text{CD}_2\text{Cl}_2$

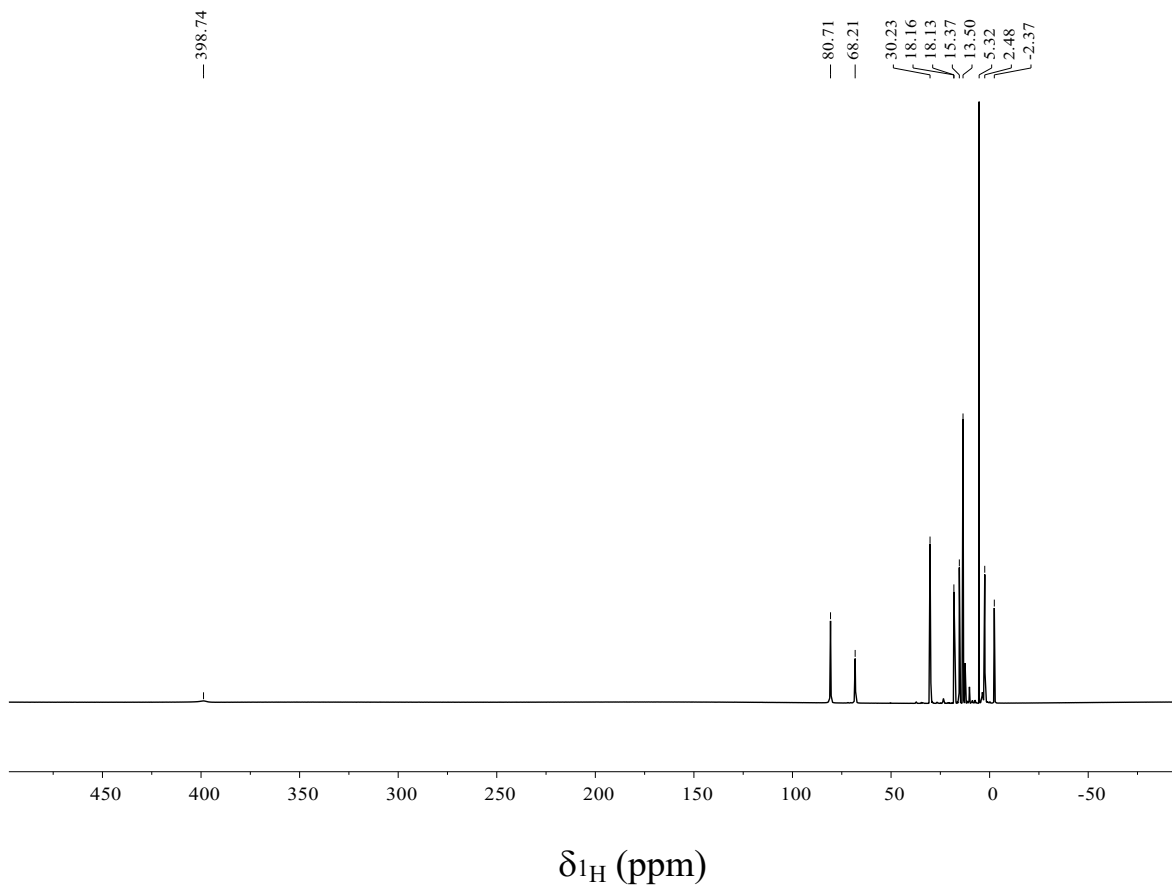


**Figure S6.** Solution  $^1\text{H}$  NMR spectrum of the complex  $[\text{Co}(\text{AcPyOx})_3(\text{BC}_6\text{H}_4\text{CH}_2\text{SSO}_2\text{CH}_3)](\text{ClO}_4)$  (**3**) in  $\text{CD}_2\text{Cl}_2$

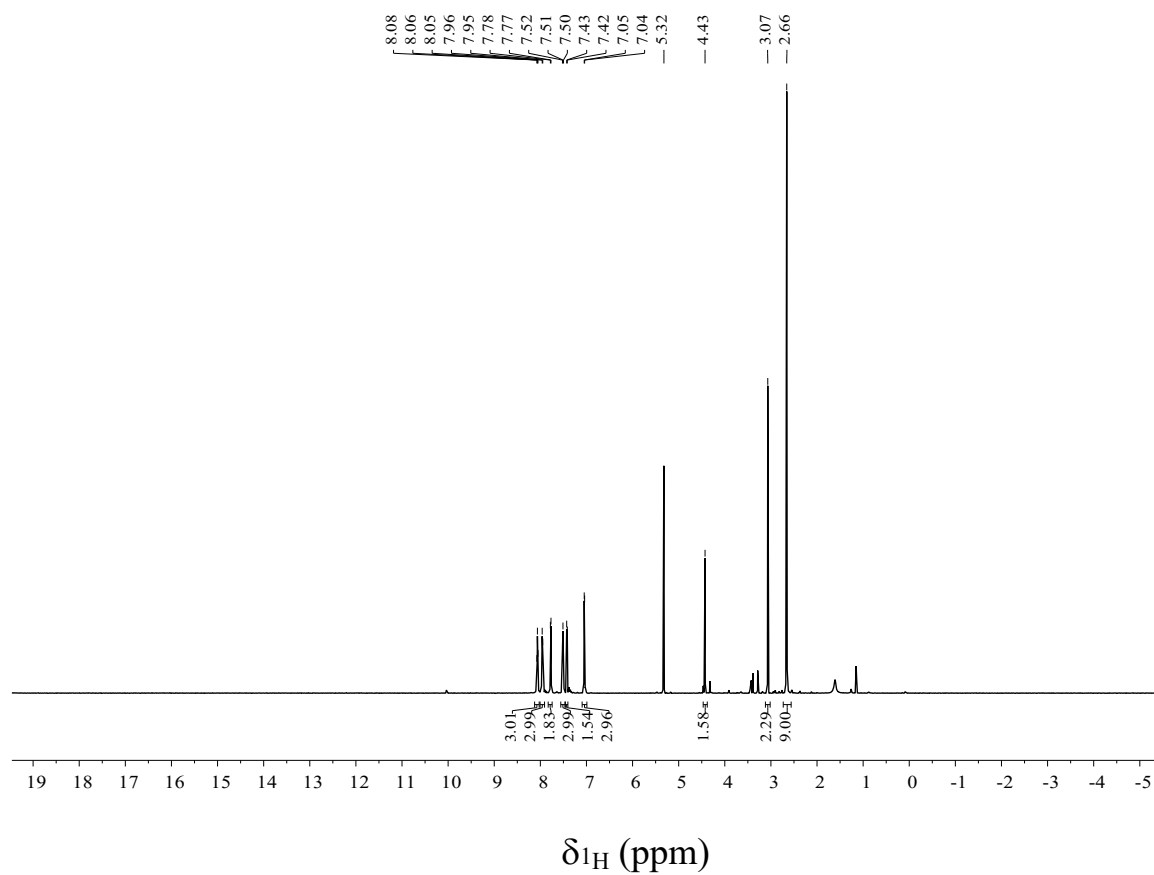


**Figure S7.** Solution  $^1\text{H}$  NMR spectrum of the complex  $[\text{Fe}(\text{AcPyOx})_3(\text{BC}_6\text{H}_4\text{CH}_2\text{SSO}_2\text{CH}_3)](\text{ClO}_4)$  (**4**) in  $\text{CD}_2\text{Cl}_2$

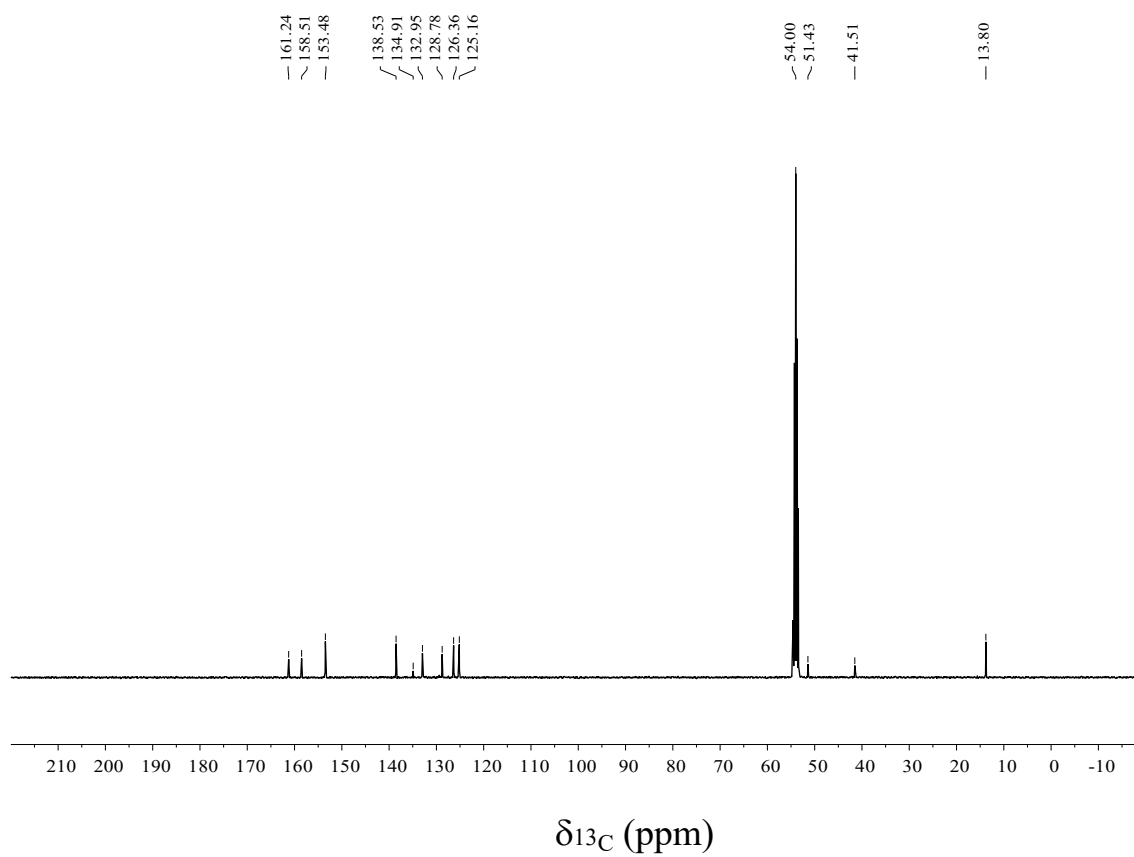


**Figure S8.** Solution  $^{13}\text{C}\{^1\text{H}\}$  NMR spectrum of the complex  $[\text{Fe}(\text{AcPyOx})_3(\text{BC}_6\text{H}_4\text{CH}_2\text{SSO}_2\text{CH}_3)](\text{ClO}_4)$  (**4**) in  $\text{CD}_2\text{Cl}_2$

Decreasing in temperature

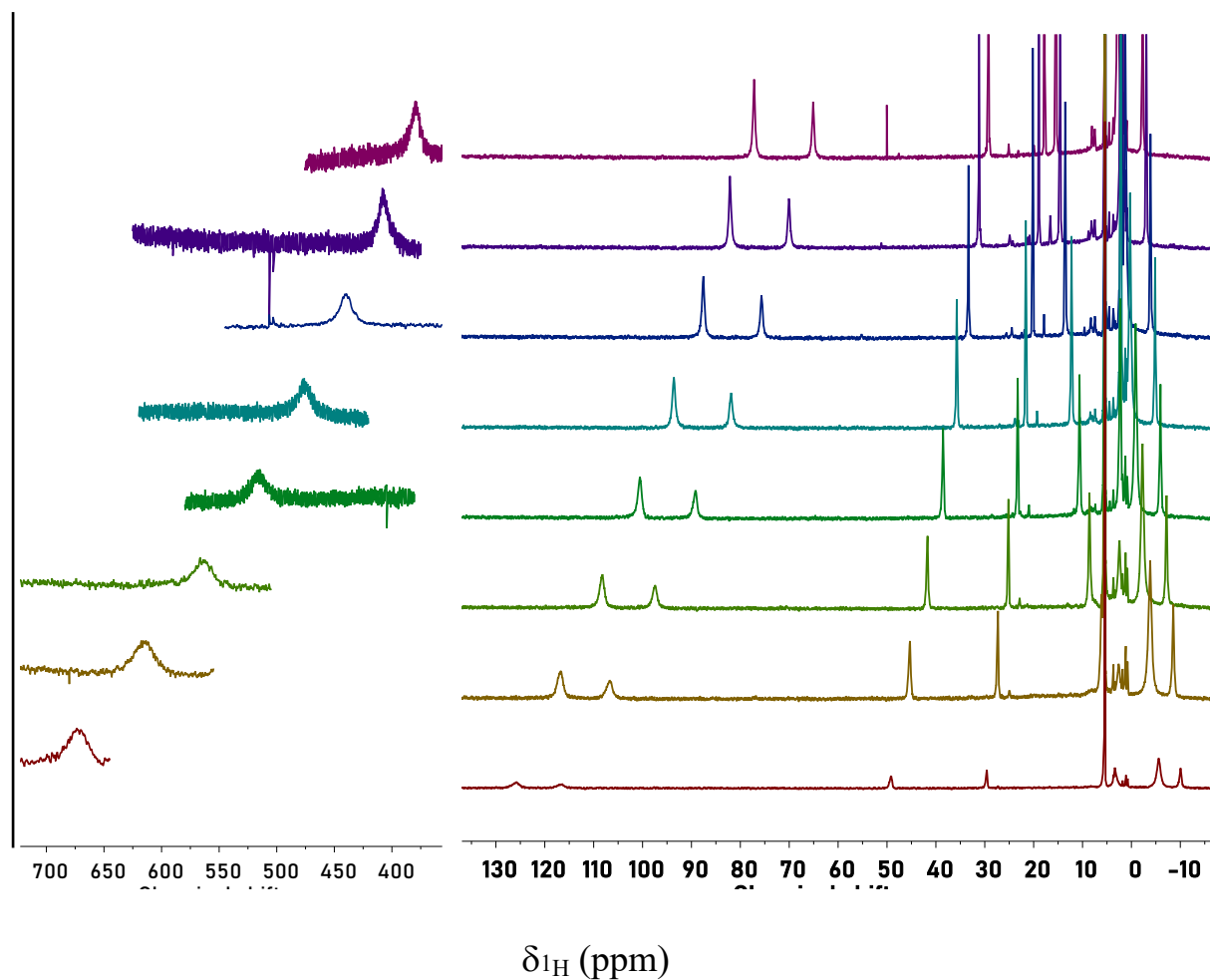


**Figure S9.** Solution  $^1\text{H}$  NMR spectra of the complex  $[\text{Co}(\text{AcPyOx})_3(\text{BC}_6\text{H}_4\text{CH}_2\text{Br})](\text{ClO}_4)$  (**1**) in  $\text{CD}_2\text{Cl}_2$  at 195, 210, 225, 340, 255, 270, 285 and 300 K, respectively. These spectra are divided into two subparts in order to clearly show the strongly shifted signal.

Decreasing in temperature

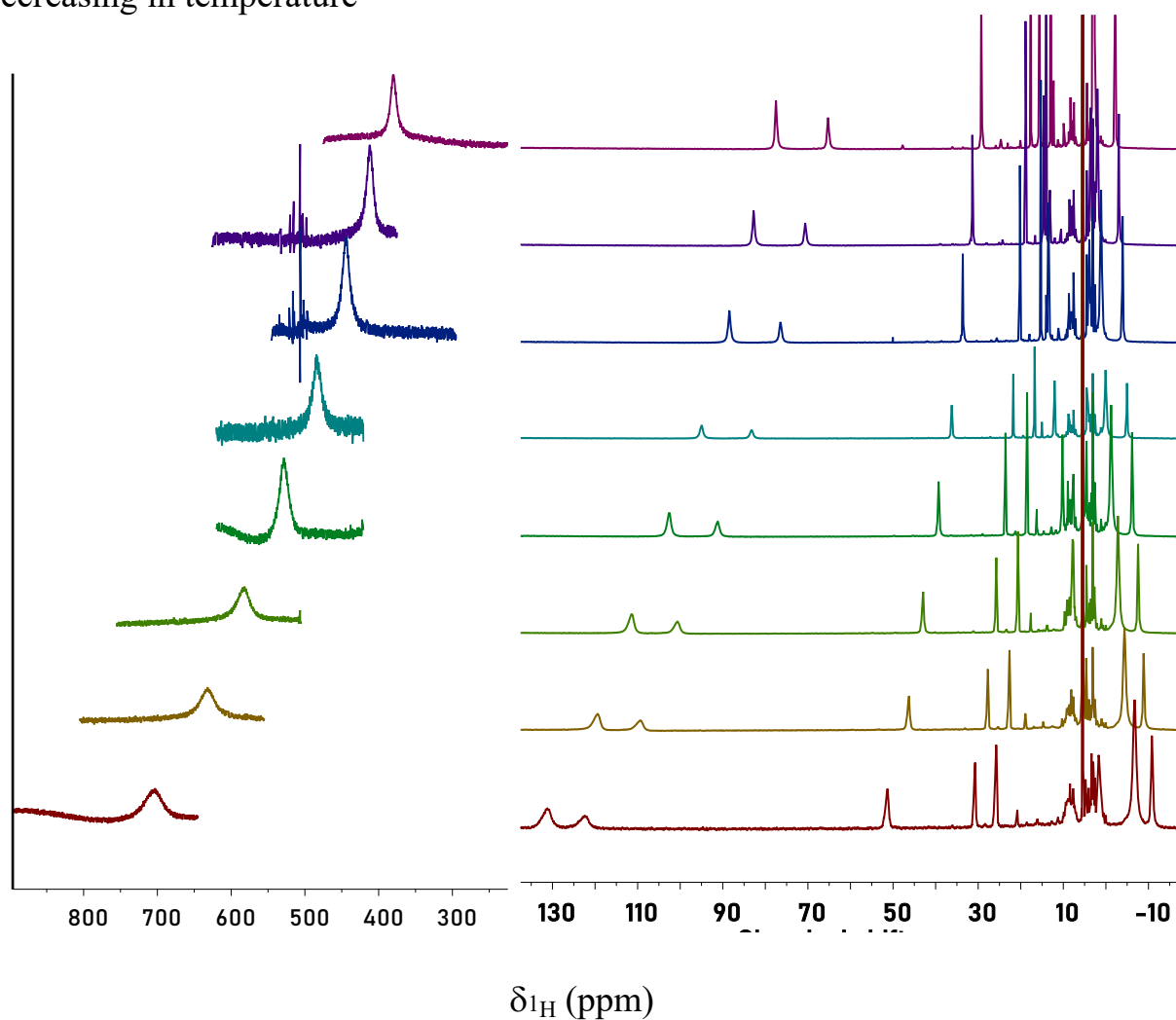


**Figure S10.** Solution  $^1\text{H}$  NMR spectra of the complex  $[\text{Co}(\text{AcPyOx})_3(\text{BC}_6\text{H}_4\text{CH}_2\text{SSO}_2\text{CH}_3)](\text{ClO}_4)$  (**3**) in  $\text{CD}_2\text{Cl}_2$  at 195, 210, 225, 340, 255, 270, 285 and 300 K, respectively. These spectra are divided into two subparts in order to clearly show the strongly shifted proton.

Decreasing in temperature

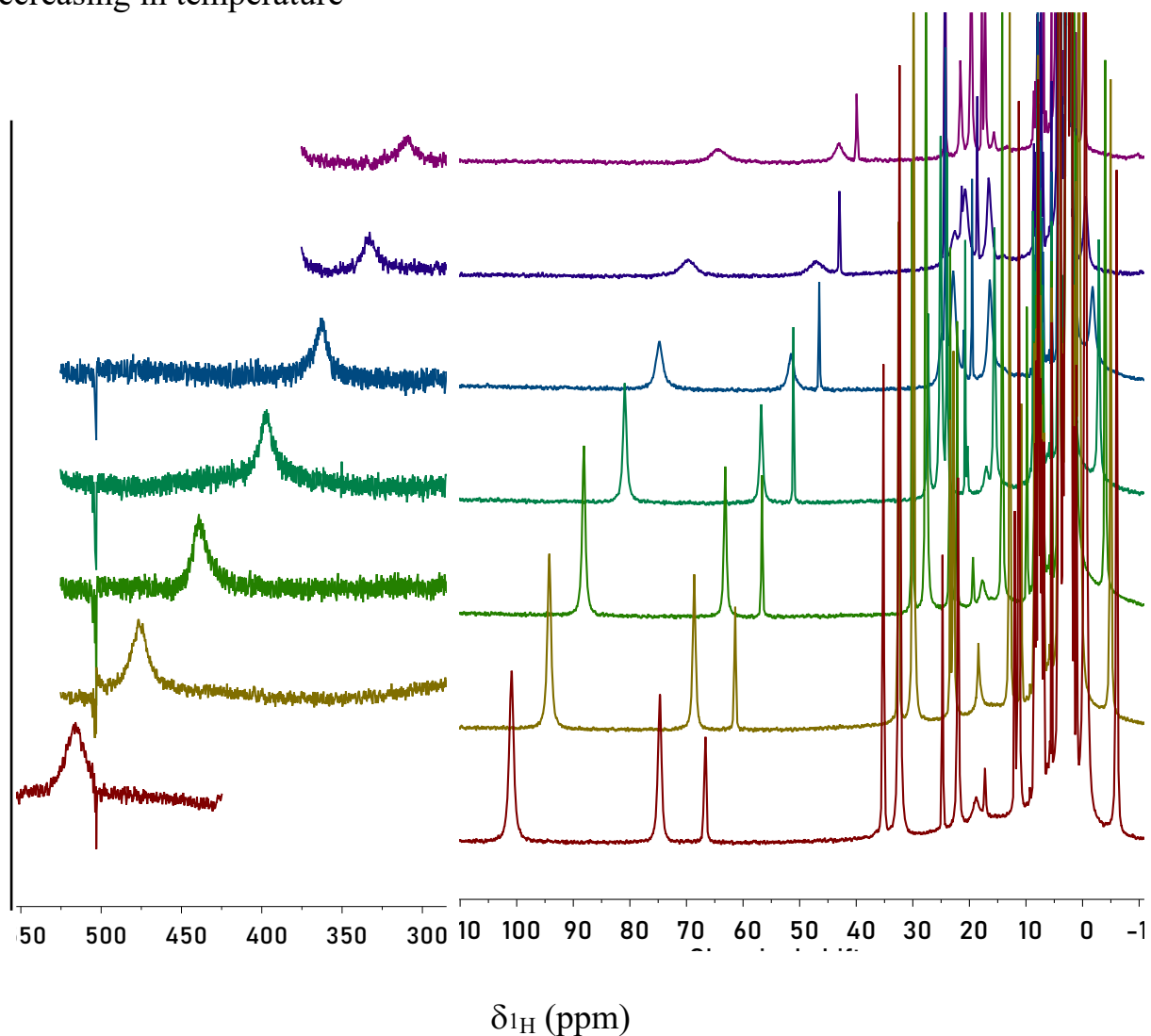


**Figure S11.** Solution  $^1\text{H}$  NMR spectra of the complex  $[\text{Co}(\text{AcPyOx})_3(\text{BFc})](\text{ClO}_4)$  (5) in  $\text{CD}_3\text{CN}$  at 235, 350, 265, 285, 305, 325 and 345 K, respectively. These spectra are divided into two subparts in order to clearly show the strongly shifted signal. The artefact at approximately 500 ppm is caused by the instrumental features.

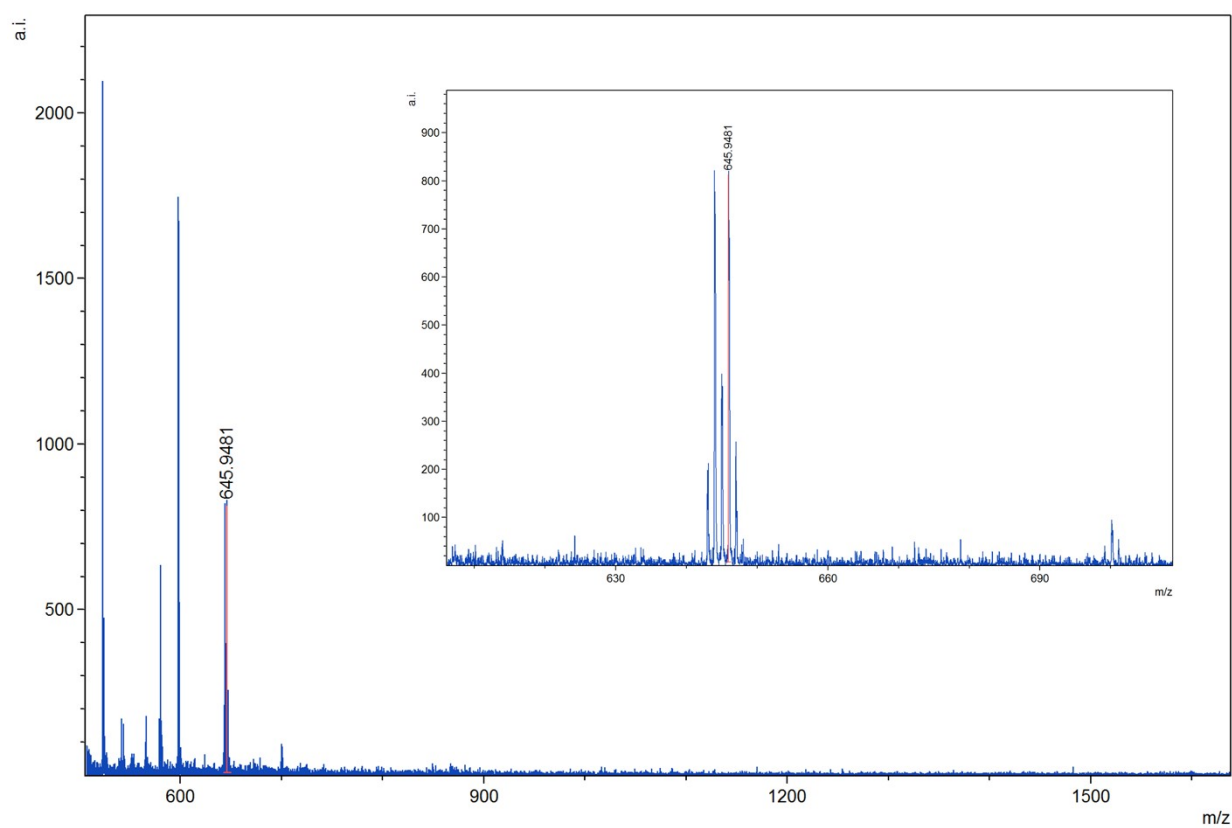


**Figure S12.** MALDI-TOF mass spectrum of the complex  $[\text{Co}(\text{AcPyOx})_3(\text{BC}_6\text{H}_4\text{CH}_2\text{Br})](\text{ClO}_4)$  (**1**) in the positive range. Inset: the characteristic peak of its pseudoclathrochelate monocation

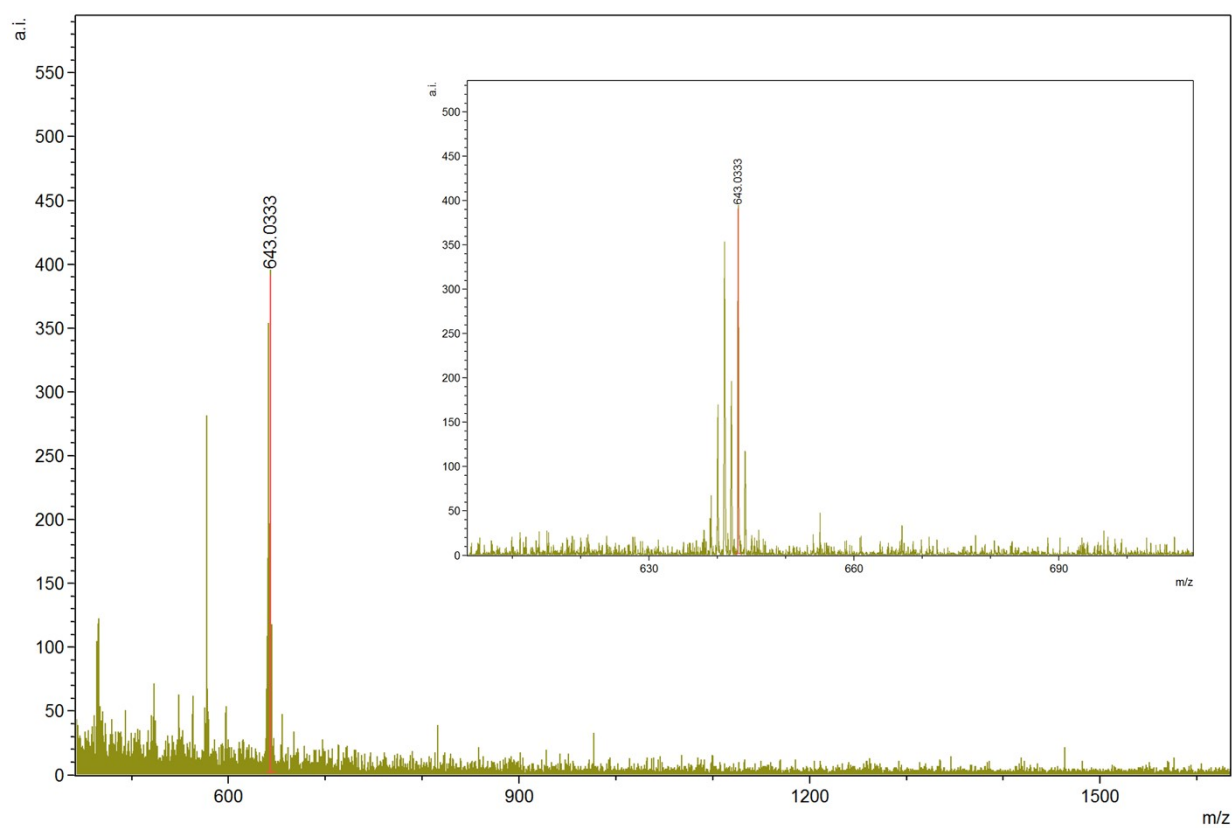


**Figure S13.** MALDI-TOF mass spectrum of the complex  $[\text{Fe}(\text{AcPyOx})_3(\text{BC}_6\text{H}_4\text{CH}_2\text{Br})](\text{ClO}_4)$  (**2**) in its positive range. Inset: the characteristic peak of its pseudoclathrochelate monocation.

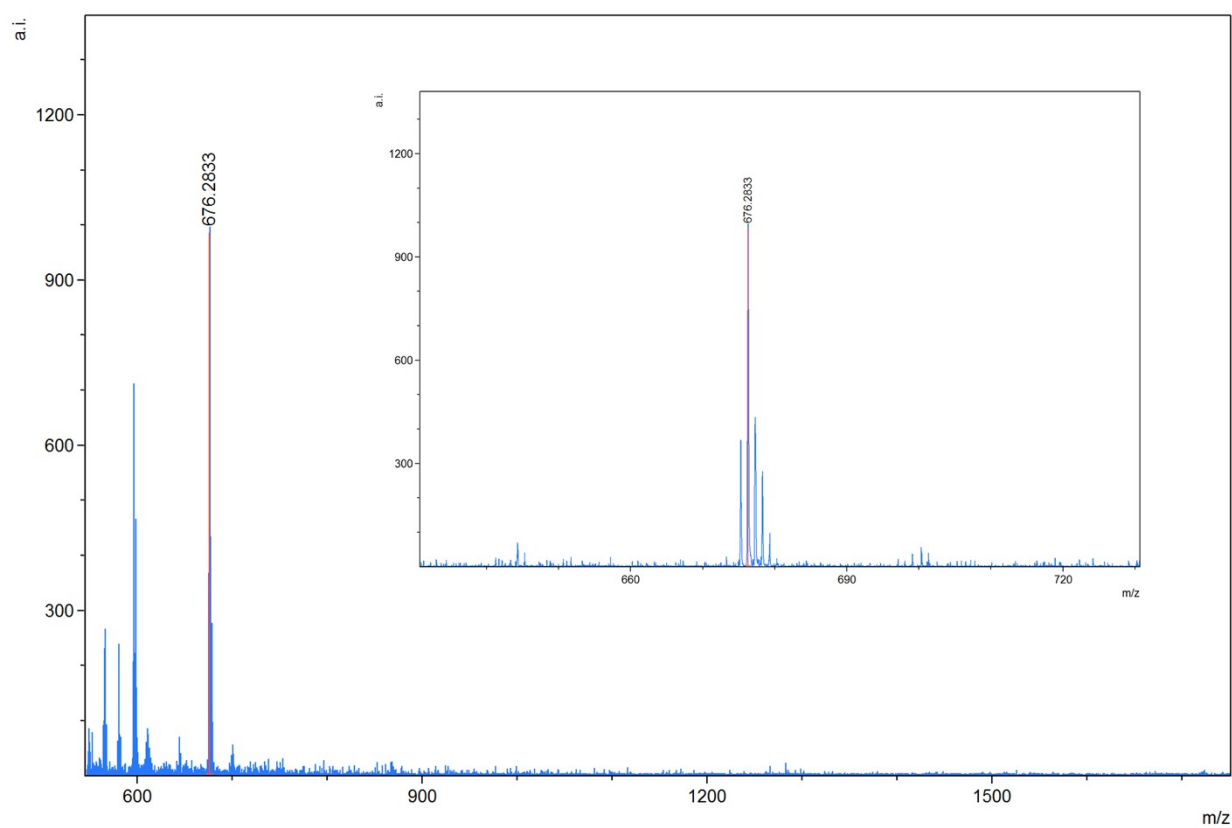


**Figure S14.** MALDI-TOF mass spectrum of the complex  $[\text{Co}(\text{AcPyOx})_3(\text{BC}_6\text{H}_4\text{CH}_2\text{SSO}_2\text{CH}_3)](\text{ClO}_4)$  (**3**) in its positive range. Inset: the characteristic peak of its pseudoclathrochelate monocation.

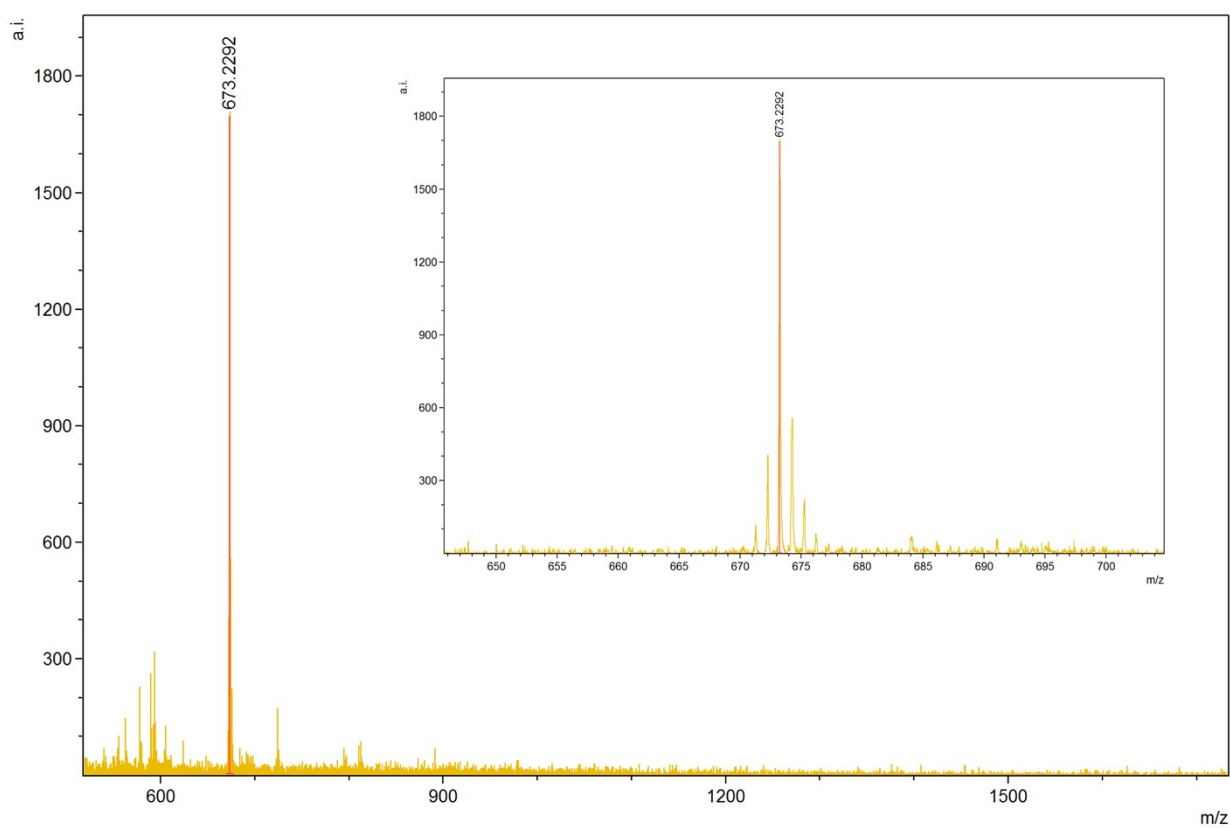


**Figure S15.** MALDI-TOF mass spectrum of the complex  $[\text{Fe}(\text{AcPyOx})_3(\text{BC}_6\text{H}_4\text{CH}_2\text{SSO}_2\text{CH}_3)](\text{ClO}_4)$  (**4**) in its positive range. Inset: the characteristic peak of its pseudoclathrochelate monocation.

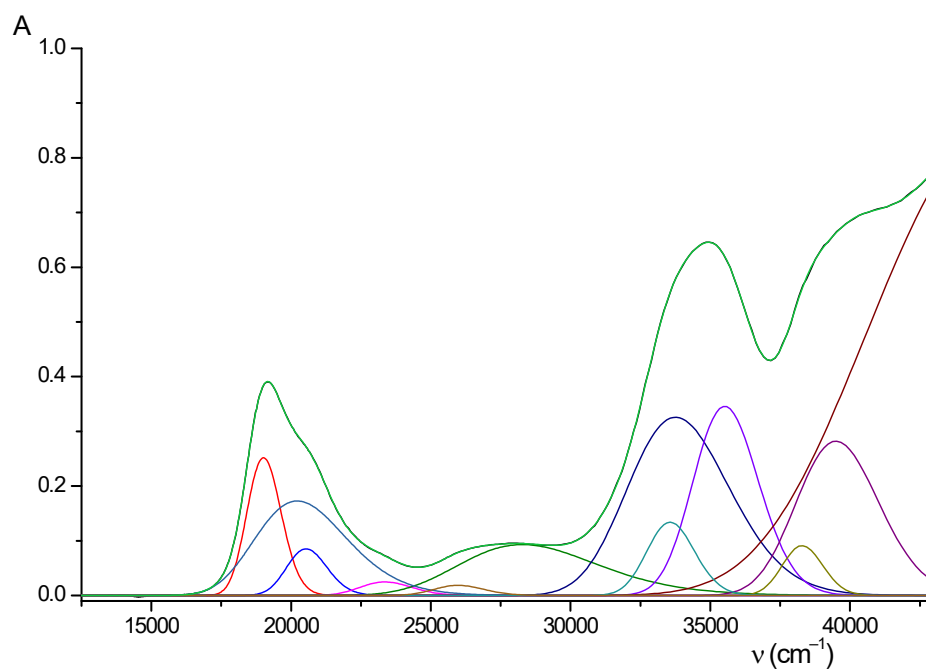


**Figure S16.** Solution UV-vis spectrum of the pseudoclathrochelate  $[\text{Fe}(\text{AcPyOx})_3(\text{BC}_6\text{H}_4\text{CH}_2\text{Br})](\text{ClO}_4)$  in  $\text{CH}_2\text{Cl}_2$  (shown in black line) and its deconvolution into the Gaussian components (shown in color lines).

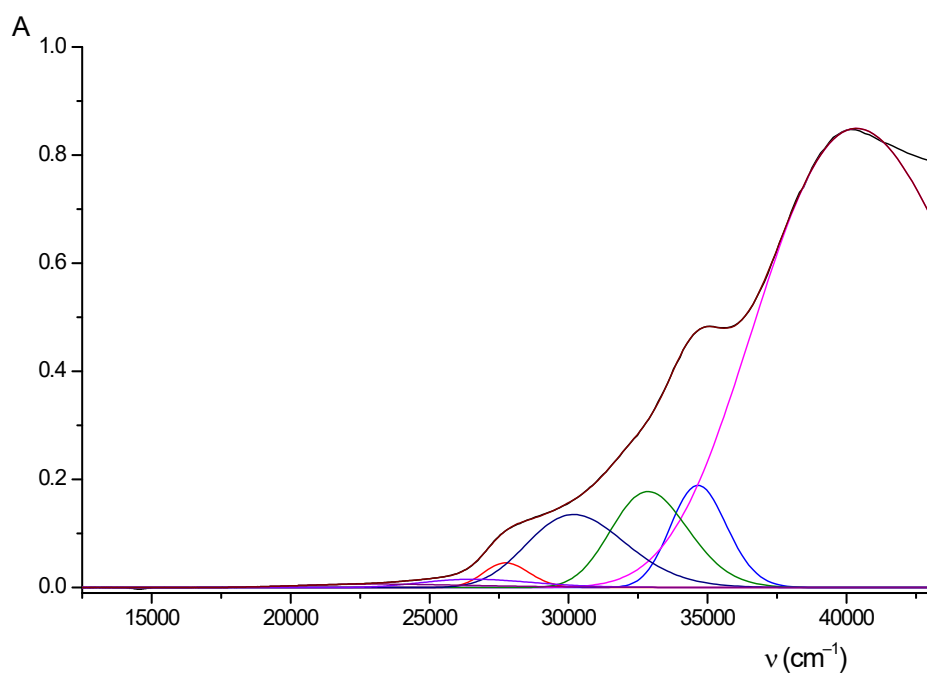


**Figure 17.** Solution UV-vis spectrum of the pseudoclathrochelate  $[\text{Co}(\text{AcPyOx})_3(\text{BC}_6\text{H}_4\text{CH}_2\text{Br})](\text{ClO}_4)$  in  $\text{CH}_2\text{Cl}_2$  (shown in black line) and its deconvolution into the Gaussian components (shown in color lines).

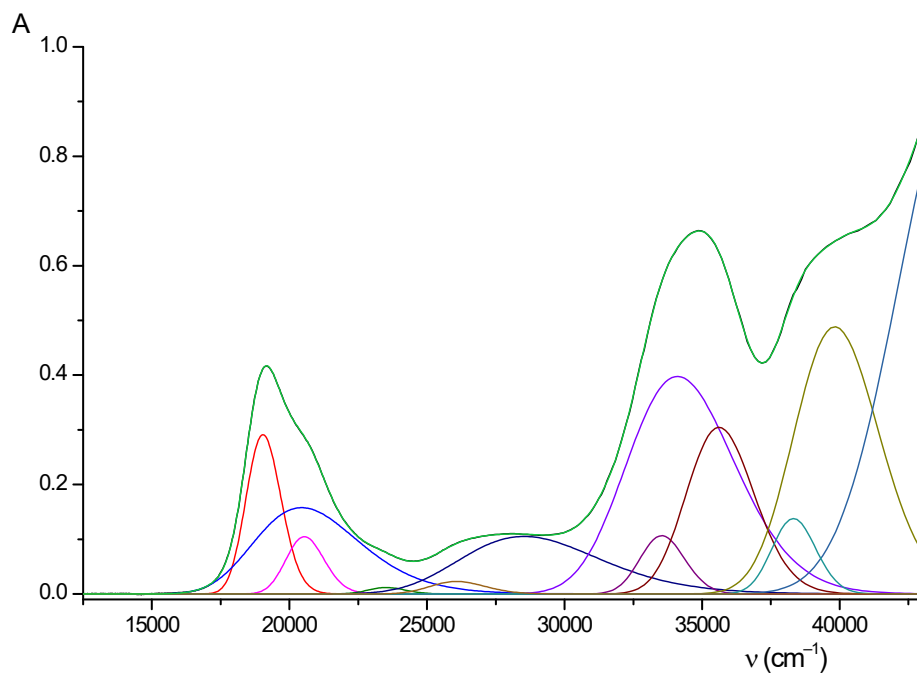


**Figure 18.** Solution UV-vis spectrum of the pseudoclathrochelate  $[\text{Fe}(\text{AcPyOx})_3(\text{BC}_6\text{H}_4\text{CH}_2\text{SSO}_2\text{CH}_3)](\text{ClO}_4)$  in  $\text{CH}_2\text{Cl}_2$  (shown in black line) and its deconvolution into the Gaussian components (shown in color lines).

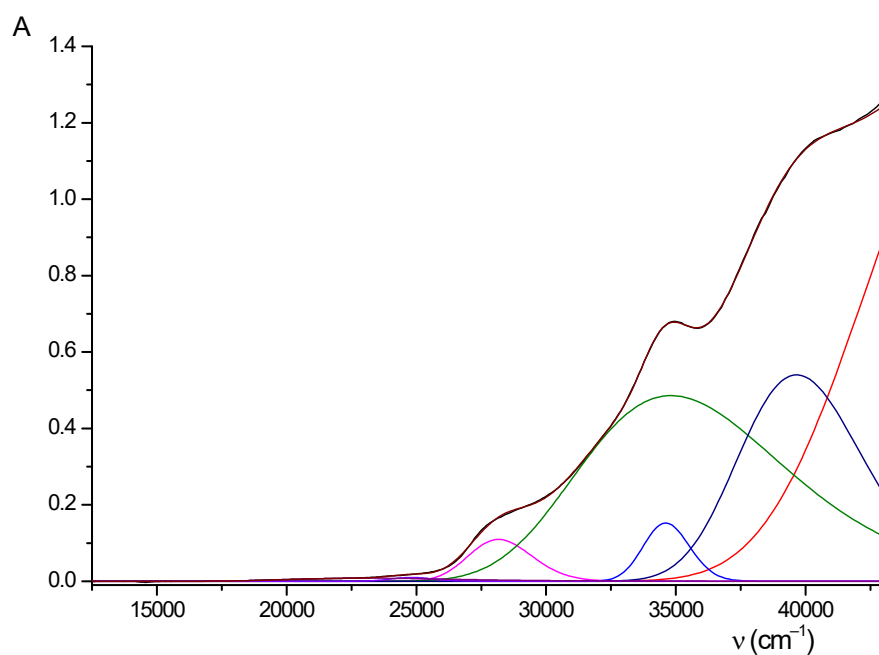


**Figure S19.** Solution UV-vis spectrum of the pseudoclathrochelate  $[\text{Co}(\text{AcPyOx})_3(\text{BC}_6\text{H}_4\text{CH}_2\text{SSO}_2\text{CH}_3)](\text{ClO}_4)$  in  $\text{CH}_2\text{Cl}_2$  (shown in black line) and its deconvolution into the Gaussian components (shown in color lines).

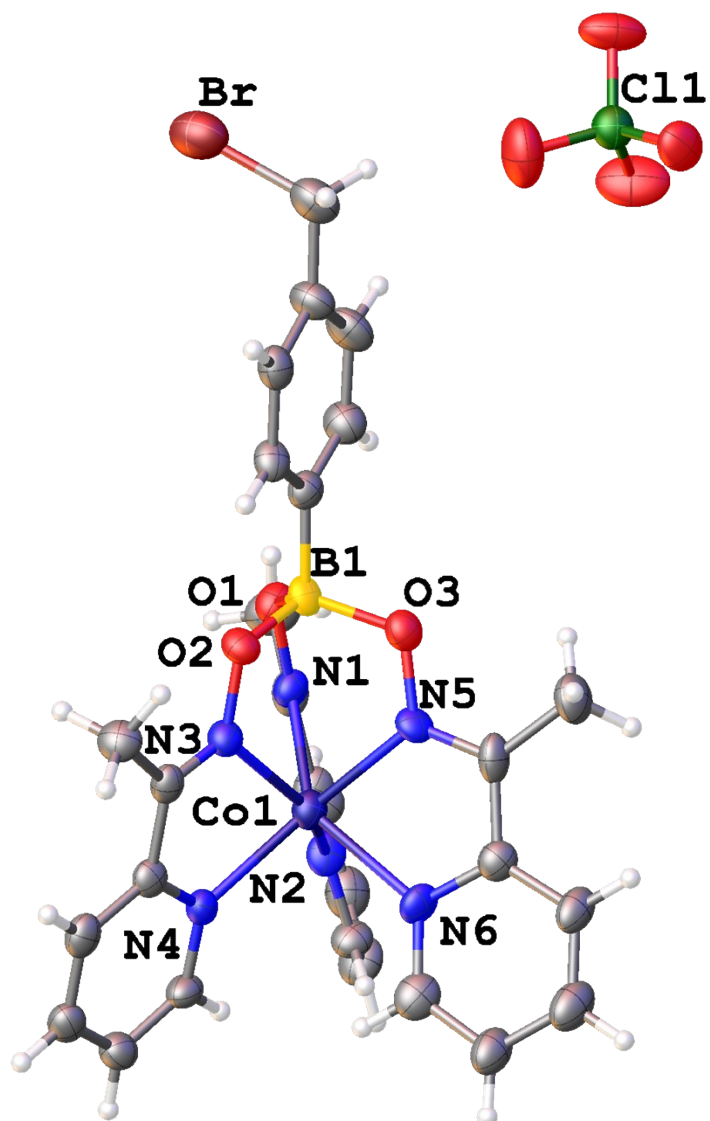


**Figure S20.** General view and numbering of atoms for the complex [Co(AcPyOx)<sub>3</sub>(BC<sub>6</sub>H<sub>4</sub>CH<sub>2</sub>Br)](ClO<sub>4</sub>) (**1**). The thermal ellipsoids are shown at 50% probability. Dichloromethane solvent molecules are omitted for clarity.

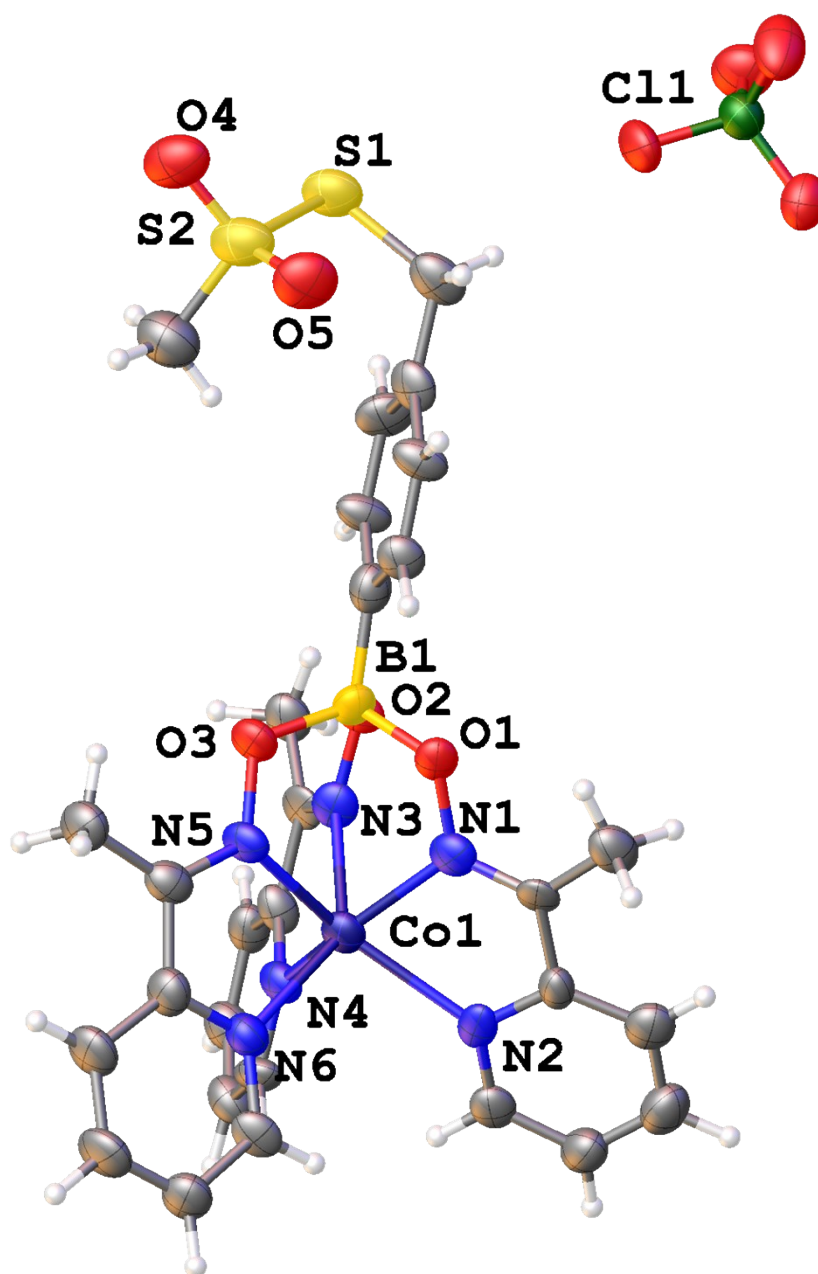


**Figure S21.** General view and numbering of atoms for the molecule [Co(AcPyOx)<sub>3</sub>(BC<sub>6</sub>H<sub>4</sub>CH<sub>2</sub>SSO<sub>2</sub>CH<sub>3</sub>)](ClO<sub>4</sub>) (**3**). The thermal ellipsoids are shown at 50% probability. Dichloromethane solvent molecules are omitted for clarity.

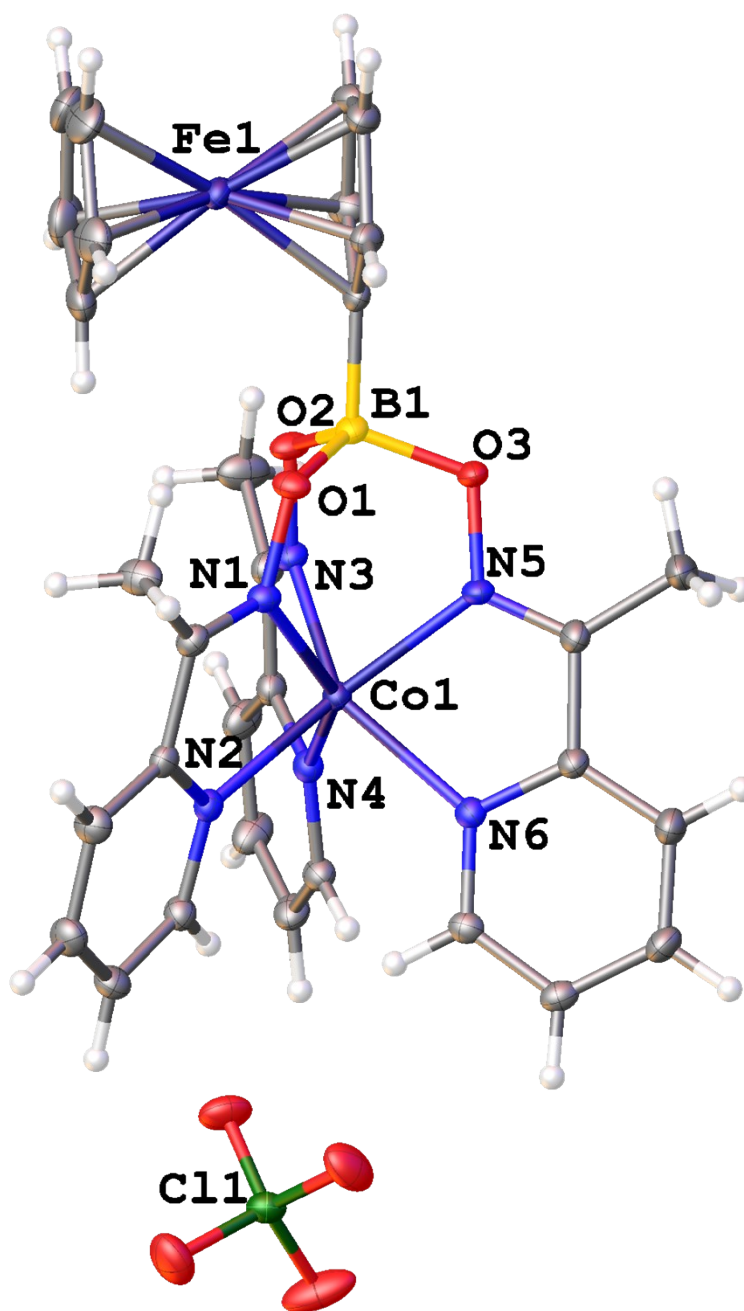


**Figure S22.** General view and numbering of atoms for the molecule [Co(AcPyOx)<sub>3</sub>(BFc)](ClO<sub>4</sub>) (**5**). The thermal ellipsoids are shown at 50% probability. Benzene solvent molecules are omitted for clarity.

**Table S1.** Crystallographic data and refinement parameters for the apically functionalized pseudoclathrochelates cobalt(II) tris-pyridineoximates **1**, **3**, and **5**

Parameter	<b>1</b> ·CH <sub>2</sub> Cl <sub>2</sub>	<b>3</b> <sup>a</sup>	<b>5</b> ·2.5C <sub>6</sub> H <sub>6</sub>
Empirical formula	C <sub>29</sub> H <sub>29</sub> BBBrCl <sub>3</sub> CoN <sub>6</sub> O <sub>7</sub>	C <sub>29</sub> H <sub>30</sub> BClCoN <sub>6</sub> O <sub>9</sub> S <sub>2</sub>	C <sub>46</sub> H <sub>45</sub> BClCoFeN <sub>6</sub> O <sub>7</sub>
Fw	829.58	775.90	954.92
Crystal system, space group	<i>P2<sub>1</sub>/c</i>	<i>P-1</i>	<i>P-1</i>
Wavelength (Å)	0.96990 (synchrotron)	0.96990 (synchrotron)	0.71073 (Mo Kα)
Crystal size (mm)	0.05×0.04×0.03 (brown prism)	0.03×0.02×0.02 (brown prism)	0.35×0.05×0.05 (brown needle)
<i>a</i> (Å)	8.8994(18)	10.939(2)	10.3495(2)
<i>b</i> (Å)	24.847(5)	13.525(3)	13.4237(2)
<i>c</i> (Å)	15.741(3)	14.224(3)	16.9990(3)
<i>α</i> (°)	90	104.71(3)	105.3670(10)
<i>β</i> (°)	98.36(3)	112.39(3)	91.2680(10)
<i>γ</i> (°)	90	95.43(3)	105.5030(10)
V (Å <sup>3</sup> )	3443.7(12)	1838.4(9)	2183.35(7)
Z	4	2	2
<i>μ</i> (cm <sup>-1</sup> )	2.158	1.402	0.832
No. of measured, independent and observed [ <i>I</i> > 2σ( <i>I</i> )] reflections	23815/7049/3871	10450/4910/3526	10531/8588/8494
<i>R</i> <sub>int</sub>	0.1016	0.1228	0.0404
<i>R</i> [ <i>F</i> <sup>2</sup> > 2σ( <i>F</i> <sup>2</sup> )], <i>wR</i> ( <i>F</i> <sup>2</sup> ), <i>S</i>	0.0902, 0.2322, 1.082	0.0974, 0.2495, 1.014	0.0375, 0.0858, 1.018
Δρ <sub>max</sub> , Δρ <sub>min</sub> (e Å <sup>-3</sup> )	1.99, -1.37	1.35, -0.98	0.39, -0.35

<sup>a</sup> This complex was refined in a form of its dichloromethane solvate. Due to a heavy disorder of the solvent molecules, they were taken into account in the crystal structure refinement using the OLEX2 Solvent Mask routine. The volume occupied by the disordered solvent molecules was estimated as 433 Å<sup>3</sup> and the scattering power of 105 e, which corresponds to approximately one dichloromethane molecule per its formula unit.

**Table S2.** Main geometrical parameters of the apically functionalized boron-capped cobalt(II) tris-pyridineoximate moieties in complexes **1**, **3**, and **5**

Parameter	[Co(AcPyOx) <sub>3</sub> (BC <sub>6</sub> H <sub>4</sub> CH <sub>2</sub> Br)](ClO <sub>4</sub> )	[Co(AcPyOx) <sub>3</sub> (BC <sub>6</sub> H <sub>4</sub> CH <sub>2</sub> SSO <sub>2</sub> CH <sub>3</sub> )](ClO <sub>4</sub> )	[Co(AcPyOx) <sub>3</sub> (BFc)](ClO <sub>4</sub> )
Co – N (Å)	2.116 – 2.135 (6)	2.081 – 2.139 (6)	2.081 – 2.108 (16)
[oxime]	<i>av.</i> 2.123 (6)	<i>av.</i> 2.095 (6)	<i>av.</i> 2.094 (16)
N...N (Å)	2.753 – 2.843	2.713 – 2.790	2.708 – 2.780
[oxime N <sub>3</sub> -base]	<i>av.</i> 2.797	<i>av.</i> 2.770	<i>av.</i> 2.752
Co – N (Å)	2.173 – 2.189(6)	2.153 – 2.198(6)	2.156 – 2.191 (16)
[pyridine]	<i>av.</i> 2.179 (6)	<i>av.</i> 2.180 (6)	<i>av.</i> 2.169 (16)
N...N (Å)	3.131 – 3.284	3.058 – 3.297	3.084 – 3.235
[pyridine N <sub>3</sub> -base]	<i>av.</i> 3.185	<i>av.</i> 3.208	<i>av.</i> 3.165
$\varphi$ (°)	20.0	25.5	22.1
$\alpha$ (°)	73.67 – 74.31	74.20 – 74.48	73.88 – 75.08
	<i>av.</i> 74.01	<i>av.</i> 74.33	<i>av.</i> 74.52
<i>h</i> (Å)	2.54	2.54	2.52

**Table S3.** Deconvoluted solution UV-vis spectra ( $\nu$ ,  $\text{cm}^{-1}$ ,  $\epsilon \times 10^{-3}$ ,  $\text{mol}^{-1} \cdot \text{l} \cdot \text{cm}^{-1}$ ) of the apically functionalized pseudoclathrochelate iron and cobalt(II) tris-pyridineoximates

Compound	$\nu_1$	$\nu_2$	$\nu_3$	$\nu_4$	$\nu_5$	$\nu_6$	$\nu_7$	$\nu_8$	$\nu_9$	$\nu_{10}$	$\nu_{11}$
$[\text{Fe}(\text{AcPyOx})_3(\text{BC}_6\text{H}_4\text{CH}_2\text{Br})](\text{ClO}_4)$	39530 (13)	38310 (4.3)	35460 (16)	33780 (16)	33560 (6.4)	28250 (4.4)	25970 (0.9)	23360 (1.2)	20530 (4.0)	20200 (8.2)	19010 (12)
$[\text{Co}(\text{AcPyOx})_3(\text{BC}_6\text{H}_4\text{CH}_2\text{Br})](\text{ClO}_4)$	40320 (35)	34600 (7.7)	32895 (7.3)	30210 (5.5)	27700 (1.9)	26600 (0.63)	23095 (0.26)				
$[\text{Fe}(\text{AcPyOx})_3(\text{BC}_6\text{H}_4\text{CH}_2\text{SSO}_2\text{CH}_3)](\text{ClO}_4)$	39840 (18)	38310 (5.0)	35590 (11)	34130 (14)	33560 (3.9)	28490 (3.8)	26040 (0.8)	23530 (0.4)	20580 (3.8)	20410 (5.7)	19050 (11)
$[\text{Co}(\text{AcPyOx})_3(\text{BC}_6\text{H}_4\text{CH}_2\text{SSO}_2\text{CH}_3)](\text{ClO}_4)$	39680 (15)	34840 (14)	34600 (4.3)	28170 (3.1)	24810 (0.27)	22990 (0.23)					
$[\text{Co}(\text{AcPyOx})_3(\text{BFc})](\text{ClO}_4)^{\text{S11}}$	49750 (48)	45250 (25)	40160 (8.6)	38170 (2.7)	36100 (15)	29325 (5.3)	24100 (0.6)	23470 (0.8)			
$[\text{Fe}(\text{AcPyOx})_3(\text{BFc})](\text{ClO}_4)^{\text{S11}}$	50000 (80)	44250 (12)	40160 (23)	35970 (7.3)	34480 (14)	33440 (7.4)	27930 (4.7)	23200 (2.3)	21600 (5.2)	20660 (3.8)	19270 (15)

**Table S4.** Energy levels for the obtained cobalt(II) complexes in a zero magnetic field calculated with spin-Hamiltonian (2) parameters of  $\sigma = 1.19$  and  $\Delta = -1237 \text{ cm}^{-1}$

Number	Energy ( $\text{cm}^{-1}$ )
1	0
2	0
3	201.4
4	201.4
5	408.4
6	408.4
7	629.9
8	629.9
9	4051.8
10	4051.8
11	4071.6
12	4071.6

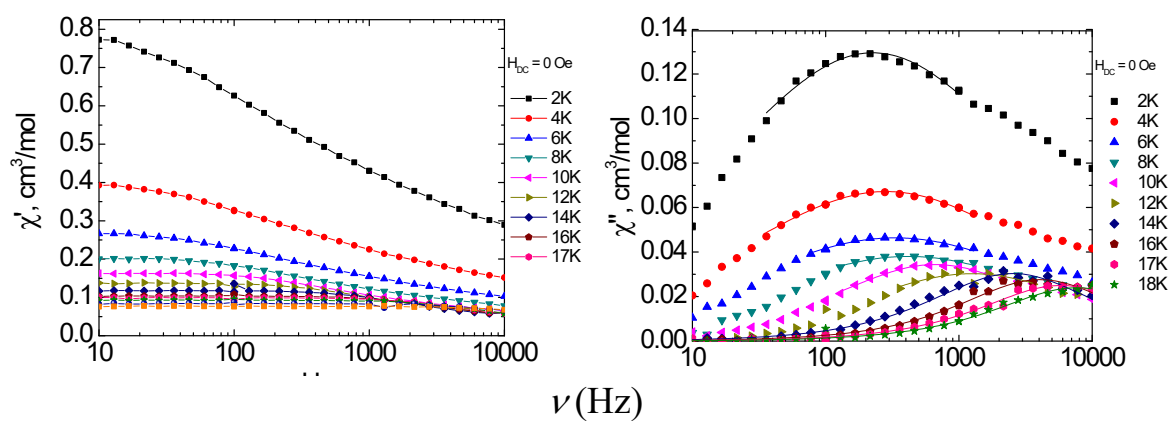


**Figure S23.** Variable-frequency in-phase ( $\chi'$ ) and out-of-phase ( $\chi''$ ) components of the ac magnetic susceptibility data for **1** in a zero dc field. The solid lines are fits by a generalized Debye model.

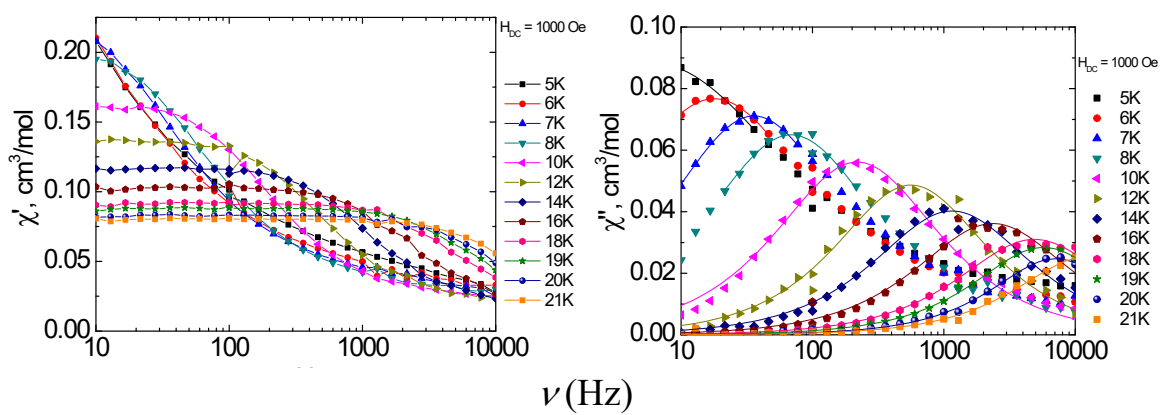


**Figure S24.** Variable-frequency in-phase ( $\chi'$ ) and out-of-phase ( $\chi''$ ) components of the ac magnetic susceptibility data for **1** in a dc field of 1000 Oe. The solid lines are fits by a generalized Debye model.

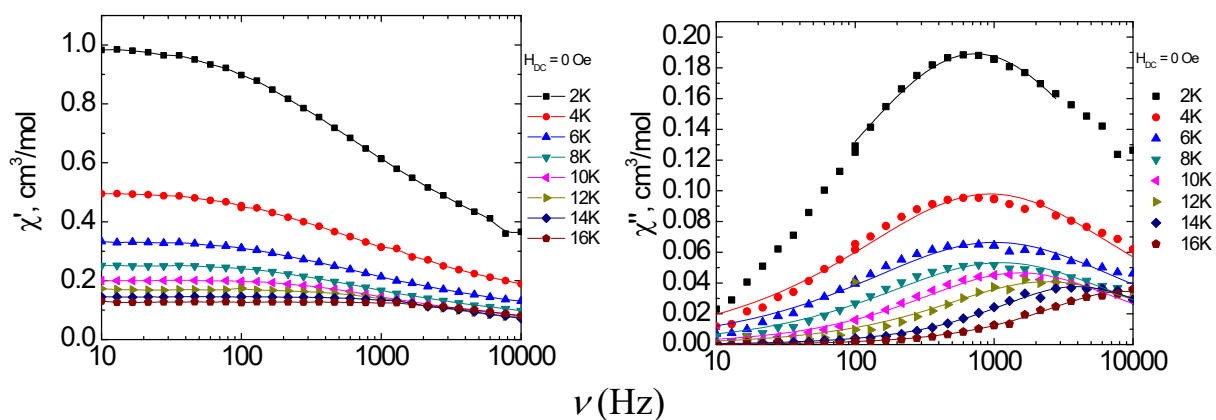


**Figure S25.** Variable-frequency in-phase ( $\chi'$ ) and out-of-phase ( $\chi''$ ) components of the ac magnetic susceptibility data for **3** in a zero dc field. The solid lines are fits by a generalized Debye model.

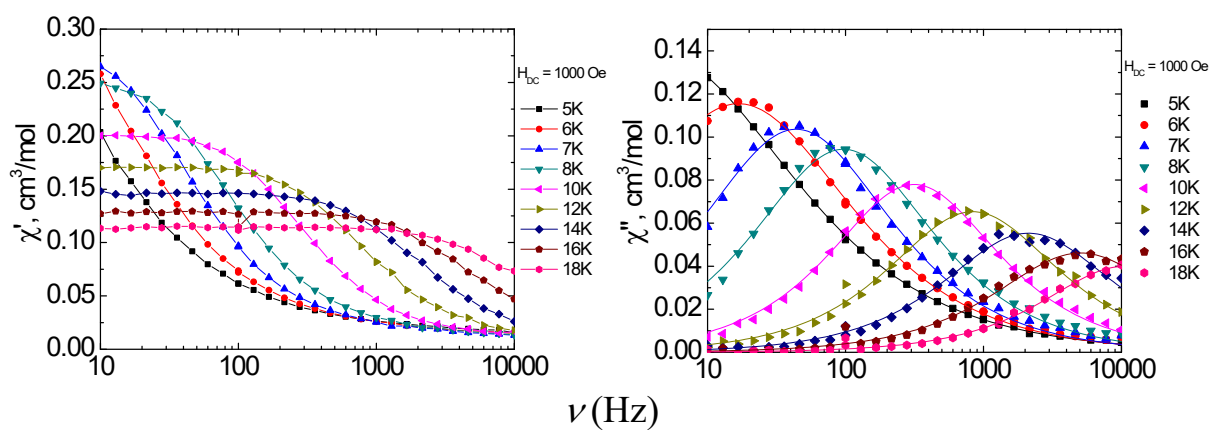


**Figure S26.** Variable-frequency in-phase ( $\chi'$ ) and out-of-phase ( $\chi''$ ) components of the ac magnetic susceptibility data for **3** in a ac field of 1000 Oe. The solid lines are fitted using a generalized Debye model.

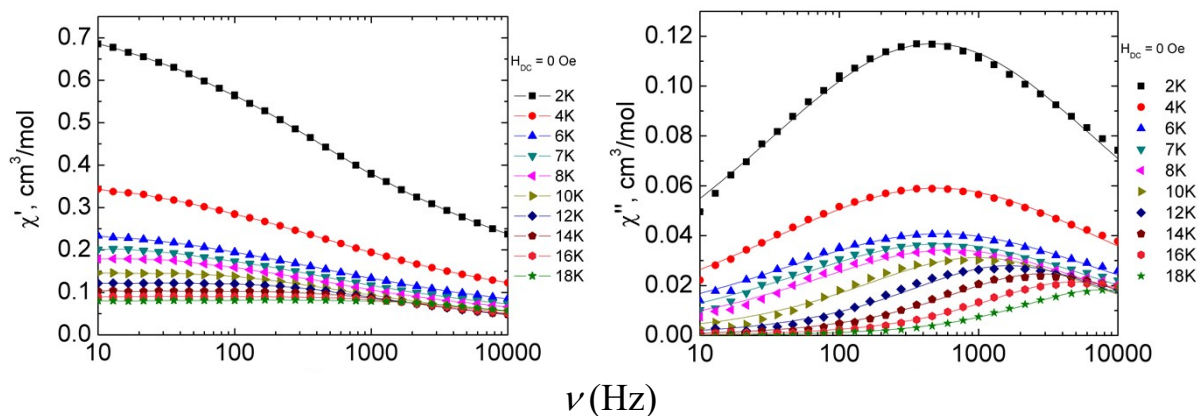


**Figure S27.** Variable-frequency in-phase ( $\chi'$ ) and out-of-phase ( $\chi''$ ) components of the ac magnetic susceptibility data for **5** in a zero dc field. The solid lines are fits by a generalized Debye model.

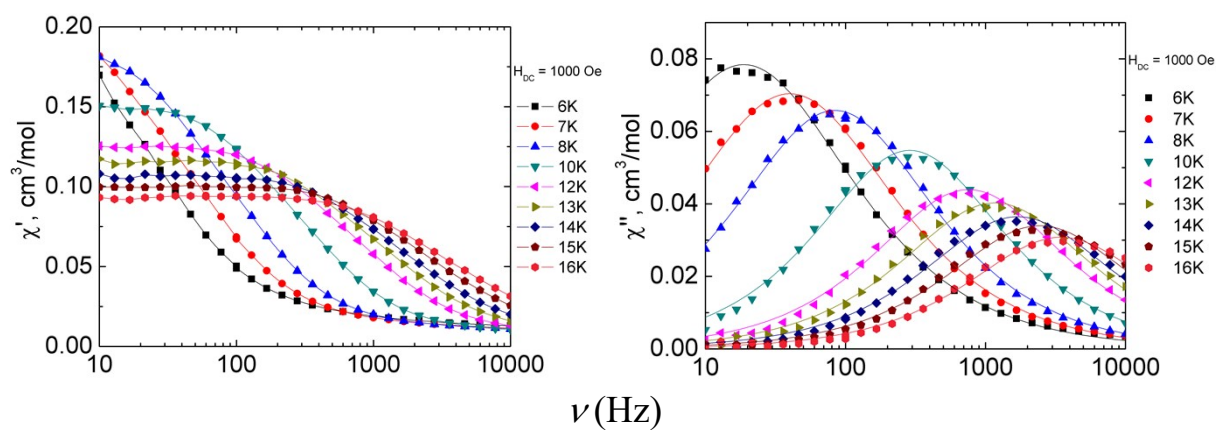


**Figure S28.** Variable-frequency in-phase ( $\chi'$ ) and out-of-phase ( $\chi''$ ) components of the ac magnetic susceptibility data for **5** in a dc field of 1000 Oe. The solid lines are fits by a generalized Debye model.

## Supporting Information References

- S1. C. B. Aakeröy, A. S. Sinha, K. N. Epa, C. L. Spartz, J. Desper, A versatile and green mechanochemical route for aldehyde–oxime conversions. *Chem. Commun.* 2012, **48**, 11289–11291.
- S2. M. Wojdyr, Fityk: a general-purpose peak fitting program. *J. Appl. Cryst.* 2010, **43**, 1126–1128.
- S3. V.A. Lazarenko, P.V. Dorovatovskii, Y.V. Zubavichus, A.S. Burlov, Y.V. Koshchienko, V.G. Vlasenko, V.N. Khrustalev, High-throughput small-molecule crystallography at the ‘belok’ beamline of the Kurchatov synchrotron radiation source: transition metal complexes with azomethine ligands as a case study, *Crystals*, 2017, **7**, 325.
- S4. R.D. Svetogorov, P.V. Dorovatovskii, V.A. Lazarenko. Belok/XSA diffraction beamline for studying crystalline samples at Kurchatov synchrotron radiation source. *Cryst. Res. Technol.* 2020, **55**, 1900184.
- S5. P. Evans, Scaling and assessment of data quality, *Acta Cryst.*, 2006, **D62**, 72 – 82.
- S6. Bruker, *Programs APEX II, version 4.0*; Bruker AXS Inc., Madison, WI, USA, 2005.
- S7. G.M. Sheldrick, SHELXT - Integrated space-group and crystal-structure determination. *Acta Cryst.*, 2015, **A71**, 3 – 8.
- S8. G.M. Sheldrick, Crystal structure refinement with SHELXL. *Acta Cryst.*, 2015, **C71**, 3 – 8.
- S9. O.V. Dolomanov, L.J. Bourhis, R.J. Gildea, J.A.K. Howard, H. Puschmann, OLEX2: a complete structure solution, refinement and analysis program. *J. Appl. Cryst.*, 2009, **42**, 339 – 341.

S10. A. B. P. Lever, *Inorganic Electronic Spectroscopy*. Elsevier: Amsterdam, The Netherlands, 1984.

S11. S.A. Belova, A.S. Belov, N.N. Efimov, A.A. Pavlov, Yu.V. Nelubina, V.V. Novikov, Y.Z. Voloshin, Synthesis, structure and magnetic properties of the ditopic ferrocenylboron-capped tris-pyridineoximate iron, cobalt and nickel(II) pseudoclathrochelates, *Rus.J.Inorg.Chem.*, 2022, **67**, 1151–1157.